Journal of Hazardous Materials 496 (2025) 139487

Contents lists available at ScienceDirect

Journal of Hazardous Materials

journal homepage: www.elsevier.com/locate/jhazmat

Methylmercury, cadmium and plastron length topologically modulate multimetallic bioaccumulation in Colombian Slider (*Trachemys callirostris* Gray, 1856): A Bayesian structure learning

Eunice Tapia-Contreras[a], Jorge Bernal-Alviz[b,*], Dora Bjedov[c,*], Álvaro Moyano- Salcedo[d], Leonomir Córdoba-Tovar[e], Jorge Buelvas-Soto[f], Atri Seña-Gaibao[a], José Marrugo-Negrete[a]

[a] *Universidad de Córdoba, Research Group in Water, Applied and Environmental Chemistry, Carrera 6 No. 77-305, Montería, Córdoba, Colombia*
[b] *St. 4A# 3S-81, Jamundí 764001, Colombia*
[c] *Josip Juraj Strossmayer University of Osijek, Department of Biology, Cara Hadrijana 8/A, Osijek 31000, Croatia*
[d] *FEHM-Lab (Freshwater Ecology, Hydrology and Management), Departament de Biologia Evolutiva, Ecologia i Ciències Ambientals, Facultat de Biologia, Universitat de Barcelona, Barcelona, Spain*
[e] *Environmental Toxicology and Natural Resources Group, Universidad Tecnológica del Chocó, Chocó, A.A. 292, Quibdó, Colombia*
[f] *Basic Sciences Faculty. Universidad de Córdoba, Cra 6 # 77-305, Montería, Córdoba 230002, Colombia*

HIGHLIGHTS

- THg medians in muscle and liver might imply potential hematotoxic risks.
- MeHg showed a homogeneous bioaccumulation in both tissues.
- 13 key positive partial conditional correlations were inferred through the BUGM.
- MeHg and Cd in muscle with PL act as multifactorial integrators of bioaccumulation.
- Bioaccumulative patterns are heterogeneous, modular, sparse and disassortative.

GRAPHICAL ABSTRACT

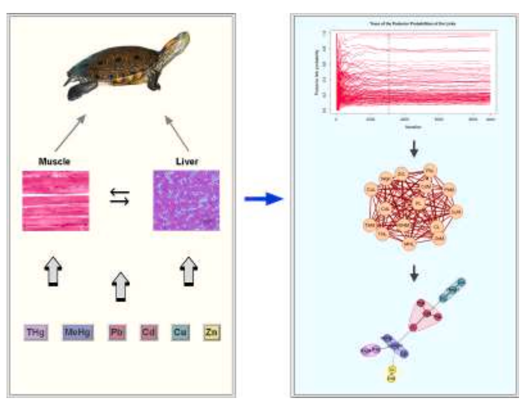

ARTICLE INFO

Keywords:
Multimetallic pollution
Chelonians
Bayesian inference
Network analysis
Environmental toxicology

ABSTRACT

Heavy metal bioaccumulation in chelonians remains relatively under-researched. Due to their high sensitivity to such type of pollution, chelonians represent ideal bioindicators for assessing aquatic ecosystems health, especially in zones with historical records of multimetallic pollution. Here, we quantified total mercury (THg), methylmercury (MeHg), lead (Pb), cadmium (Cd), copper (Cu), and zinc (Zn) in muscle and liver of *Trachemys callirostris* and examined significant differences ($p < 0.05$) between their concentrations in both tissues. As well, their partial-conditional bioaccumulative correlations along with their uncertainty in relation to carapace length (CL), plastron length (PL) and turtles' weight were determined through a Bayesian Undirected Graphical Model (BUGM). The topological co-occurrence in the inferred correlations was modelled using network analysis through

* Corresponding authors.
E-mail addresses: zeth1700@gmail.com (J. Bernal-Alviz), dora.bjedov@biologija.unios.hr (D. Bjedov).

https://doi.org/10.1016/j.jhazmat.2025.139487
Received 30 May 2025; Received in revised form 4 August 2025; Accepted 6 August 2025
Available online 7 August 2025

a weighted and undirected graph. Results reveal that median THg concentrations in muscle and liver (157.47 μg/kg and 331.78 μg/kg) were within the referenced hematotoxicity range (100 μg/kg - 350 μg/kg). MeHg was the only pollutant that showed no significant inter-tissue differences. The BUGM inferred 13 key positive associations (12.38 % of total) with a high posterior probability of correlation structure (S) ($p = 0.654$). Network analysis revealed a highly modular, heterogeneous, sparse and disassortative topology, where MeHg and Cd in muscle with PL acted as the most central and prominent nodes, bridging five well-differentiated communities. This work represents the first Bayesian approach applied to model structural bioaccumulation networks in chelonians, offering a novel framework to approach the nature and uncertainty of complex interactions between pollutants and morphometry in water ecosystems.

1. Introduction

The wetland ecosystems of northern Colombia have experienced significant pollution processes with heavy metals over the past decades. The main sources of these pollutants include mining, agricultural practices, metallurgical activities, and urban wastewater effluents [103,2,47]. Among these pollutants, particular attention has been given to total mercury (THg), methylmercury (MeHg), lead (Pb), cadmium (Cd), copper (Cu), and zinc (Zn), due to their persistent presence in such environmental matrices [36,45,63]. At the national level, studies have been conducted across various taxa and environmental compartments, including fish, amphibians, birds, reptiles, mammals, macrophytes, and sediments polluted with chemical agents [99,132,134,135,19,24,32,72]. In recent decades, research utilizing chelonians as bioindicators has increased [16,41,62,65]. Despite the advantages that chelonians offer for monitoring environmental pollution, ecotoxicological studies focusing specifically on this order remain scarce in Colombia [118,168,69].

In this context, the species *Trachemys callirostris* is a freshwater chelonian that inhabits lotic waters with low currents or lentic waters at low altitudes being endemic to northern South America, and mainly distributed in Colombia [118,130]. During the dry season, individuals migrate from streams to forests, where they seek refuge among roots or trunks [118,129]. In Colombia, *T. callirostris* is distributed across the basins of the Sinú, San Jorge, Cauca, Magdalena, Cesar, and Ranchería Rivers [129]. The exact lifespan of *T. callirostris* is not well-established but is thought to be similar to that of *Trachemys scripta* due to their phylogenetic closeness [139,59], being the lifespan of *T. scripta* approximately 30 years [64]. In this regard, *T. callirostris* represents the most exploited chelonian in Colombia for human consumption purposes [28,130,144], having its populations a vulnerable conservation status [144,21]. Regarding the primary sources of heavy metal emissions in the areas influencing the study region, ferronickel mining occurs in the Sinú River basin [8,100], while alluvial and small-scale artisanal mining (ASGM) is conducted in the Cauca and Magdalena River basins [116,131,147]. Additionally, agricultural activities contribute significantly to trace elements presence such as As, Cd, Cu, Pb, and Zn [100,101]. Given this context, *T. callirostris* may serve as an efficient bioindicator due to its feeding ecology, trophic level, lifecycle, and relative sedentary behaviour within the aquatic habitats it occupies [168,169,86].

Regarding environmental pollutants effects on chelonians, exposure to THg and MeHg tends to induce endocrine disruptions, epigenetic changes, and teratogenesis [106,109], as well as hematotoxicity, immunotoxicity, and altered enzymatic activity [42], thus these adverse effects co-occurrence is common since THg accumulation implies both MeHg and mercury (Hg) inorganic species accumulation [133]. Pollution with trace elements such as Cd triggers nephrotoxicity, decreased gametic and reproductive viability, and hepatocellular genotoxicity [48,76,84]. Similarly, Pb bioaccumulation in these reptiles has the potential to cause immunosuppression [167], neurotoxicity, behavioural changes, and reduced juvenile survival rates [23]. On the other hand, excessive accumulation of essential elements such as Cu and Zn, along with their derivatives, is associated with oxidative stress, apoptosis, alterations in gene expression, inflammatory processes, detriments in spermatogenesis, mutagenicity, and cytotoxicity [122,166,5]. These effects could act as stressors that, over the long term, threaten the stability and survival of *T. callirostris* populations and pose a public health concern for human populations that rely on this reptile in the study area [168]. Moreover, there is evidence demonstrating the occurrence of significant correlations between the bioaccumulation of pollutants such as mercury and lead, and various morphometric parameters related to growth rates, including body weight, plastron length, and carapace length, in freshwater and brackish-water turtles [141,142,23].

On the other hand, graphical models arrange probabilistic relationships structures, among variables, in which nodes correspond to variables, and the absence of edges (correlation coefficients) represents conditional independence [50]. These models enable the assessment and disentanglement of near-ground-truth co-occurrence and interaction dynamics, within complex and vast biological systems [52], and can be enhanced through Bayesian modelling to infer the most plausible underlying correlation structure from the posterior [112]. Furthermore, graphical models based on probabilistic correlations and network analyses have been successfully implemented in life-sciences fields such as genomics and ecology [107,123,39]. However, their application in assessing pollution and bioaccumulation processes in higher organisms, such as chelonians, remains uncertain due to limited research in these reptiles [37,44,49]. Consequently, this study was aimed to:

(I) Quantify THg, MeHg, Pb, Cd, Cu, and Zn accumulation in the muscle and liver of *T. callirostris*.
(II) Assess inter-tissue accumulative differences for each pollutant.
(III) Determine probabilistic partial conditional associations between muscular and hepatic THg, MeHg, Pb, Cd, Cu and Zn accumulation, with turtles' carapace length (CL), plastron length (PL) and weight using a Bayesian Undirected Graphical Model (BUGM).
(IV) Analyse structural and topological co-occurrence of THg, MeHg, Pb, Cd, Cu, and Zn accumulation in muscle and liver in relation to CL, PL and weight through a network analysis.

2. Materials and methods

2.1. Study area

La Mojana is a subregion located in the Momposina Depression in north-western Colombia, covering approximately 5545 km^2. This territory, characterized by extensive alluvial plains and lowlands, consists of numerous swamps, small streams, and more than 50 urban settlements. The study area is notable for its rich biodiversity, structured by a wetland complex fed by three major rivers: the San Jorge, the Magdalena, and the Cauca [25,3]. Its climate is warm and humid, with annual mean temperatures ranging between 28 °C and 33 °C [99,101]. La Mojana is an interior delta where the Magdalena, Cauca, and San Jorge rivers converge [115]. This intricate wetland complex includes marshes, channels, meanders, streams, swamps, and seasonally flooded forests, all interconnected through biological corridors formed by tributaries and their channels. The region's alluvial plains provide critical habitats for numerous species, including fish, local and migratory birds, reptiles, mammals, and amphibians [150]. In fact, La Mojana is recognized as

Colombia's largest floodplain [10,9]. In this sense, the study area was specifically delimited to the wetlands complex and largest swamps in the influence zones of San Marcos, San Benito Abad, and Sucre municipalities, located in the Sucre department on the southwestern margin of the interior delta. Thus, the influence zones of San Marcos municipality comprise La Cruz and Las Flórez swamps, while in the influence zones of San Benito Abad municipality are found the Doña Luisa and Grande de San Benito swamps, as well the influence zone of Sucre municipality encompasses the Mogua and Grande swamps (Fig. 1).

From April to December, these rivers cause seasonal flooding that significantly influences hydrological cycles, transporting and dispersing substantial pollutant loads, including mining residues, into ecosystem matrices. These pollutants originate upstream in the Cauca River and San Jorge River basins, areas with intense ASGM activities [105]. Additionally, agricultural and industrial activities in the San Jorge, Magdalena, and Cauca River basins, alongside local agricultural practices, are among the main sources of emissions and pollution in the study area with trace elements such as Pb and Cd, and essential elements like Cu and Zn [100,101].

2.2. Capture, identification of *T. callirostris* and sample collection

The studied species was collected from the six characterized swamps in the influence areas of San Marcos, San Benito Abad and Sucre municipalities by ancestral subsistence fishers between June 2022 and August 2022. Individuals were collected at the usual capture and fishing sites of this species, which represent their transit and feeding/foraging zones in each of the six major swamps and their associated water bodies, with these sites characterized by slow-moving waters with clay-silt bottoms and an important number of macrophytes [130,43]. Collections were conducted accompanied by local fishermen in each of the six major swamps, where the fishermen used trammel nets measuring 1 m high × 6 m wide for 10 passes per sampling, in areas of moderate depth with few submerged objects, for 4 h per sampling [154]. A total of $n = 23$ unsexed adult specimens were collected and identified based on the taxonomic criteria described in the *Libro Rojo de Reptiles de Colombia* [114]. For each individual *T. callirostris* weight was recorded with a precision of ± 0.1 g using a digital scale, and the PL, as well as CL, were measured in centimetres with a precision of ± 1 mm using a digital calliper. Muscle and liver tissue samples were obtained by fishers using latex gloves under the inspection of the field researchers immediately after sacrificing each individual in accordance with the handling and dissection protocol for chelonians described by Wyneken [163], in this way the samples were obtained using a previously sterilized stainless-steel scalpel, ensuring each pair of tissue samples came from the same individual to avoid pseudoreplication. Fresh liver and muscle samples ranging from 6 – 16 g were collected following the protocols outlined by Yu et al. [167] and rinsed four times with ultrapure water to remove impurities and avoid tissue cross-contamination [1]. Once rinsed, samples were then immediately placed in sterile polypropylene tubes and stored at −20°C for subsequent treatment [75] and transported to the Toxicology and Environmental Management Laboratory at the University of Córdoba.

2.3. Determination of THg and MeHg

Total mercury (THg) concentrations in the muscle and liver tissues of *T. callirostris* were determined using the US-EPA 7473 method [151]: mercury in solids and solutions by thermal decomposition, amalgamation, and atomic absorption spectrophotometry (TDA-AAS). The analysis was conducted using a DMA-80 TRICELL direct mercury analyser (Milestone Inc., Italy). The certified reference material used was DORM-2 (4640 ± 260 μg/kg) from the National Research Council of Canada (NRCC). In this way, the detection limit was 5 μg/kg, and the quantification limit was 10 μg/kg. Analyses were performed in triplicate and calibrated against the standard deviations of blanks, achieving a mean recovery of 97 % for both tissues with coefficients of variation (CV) greater than 5 %. THg concentrations were reported in μg/kg of wet weight (w. w.) **(Table SI-1)**.

MeHg concentrations were determined in approximately 500 mg of muscle and liver tissue samples, weighed into polytetrafluoroethylene (PTFE) tubes, volume of 3 mL of a 25 % methanolic KOH solution was used to extract MeHg. The extraction was carried out in an oven at 70 °C for 8 h in a in a closed MILESTONE ETHOS 1 microwave digestion system [26]. Samples were kept away from light sources to prevent MeHg transformations. Subsequently, an ethylation process was performed by adding 500 μL of a 2 mol/L acetate buffer, followed by 30 μL of the sample and 50 μL of 1 % tetraethyl borate, while the final volume was adjusted to 50 mL with deionized water. A solid phase microextraction (SPME) fibre was immersed in the samples for 15 min at 40 °C to extract methylmercury, subsequently the fibre was inserted into a GC autosampler TD-100 (Markes International Ltd., United Kingdom) and passed to a TRACE 1310 gas chromatographer (Thermo Scientific - US) coupled with an ISQ 7000 Single Quadrupole Mass Spectrometer (Thermo Scientific – US) for MeHg quantification via Thermal Desorption Gas Chromatography-Mass Spectrometry (TD-GC-MS) [125]. Muscle and liver samples were validated in triplicate (CV > 5 %), and the certified reference material employed was BCR-463 (3040 ± 160 μg/kg) from the Joint Research Centre (JRC, EU). MeHg quantification in muscle and liver samples yielded an average recovery rate of 98 %, with detection and quantification limits set at 15 μg/kg and 20 μg/kg, respectively. MeHg concentrations were recorded in μg/kg of w. w. **(Table SI-1)**.

2.4. Determination of Pb, Cd, Cu, and Zn

Cd, Pb, Cu, and Zn quantities in muscle and liver tissues of *T. callirostris* were measured using graphite furnace atomic absorption spectrophotometry (GFAAS). A Thermo Scientific iCE 3500 furnace was employed, following the US-EPA 3051 A (SW-846) method [152]. An acid digestion of 0.5 g of muscle and liver tissue was performed using an HNO_3 and HCl solution (3:1, v/v) in a closed environment using a MILESTONE ETHOS 1 microwave digestion system for 4 h at 95 °C [34]. Quality control was carried out in triplicate, using the certified reference material DORM-2 from the NRCC. Detection limits were established at 1 μg/kg for Cd, 3 μg/kg for Pb, 10 μg/kg for Cu, and 5 μg/kg for Zn, while quantification limits set at 5 μg/kg for Cd, 20 μg/kg for Pb, 50 μg/kg for Cu, and 25 μg/kg for Zn, respectively. Thus, average recovery rates for all analyses ranged from 96.6 % to 98.8 %, with their CV below 5 %. The concentrations of these elements are reported in μg/kg of w. w. **(Table SI-1)**.

2.5. Statistical treatment

2.5.1. Descriptive and multivariate analysis

The distributions of weight, PL, and CL, along with the muscle and liver concentrations of THg, MeHg, Pb, Cd, Cu, and Zn in *T. callirostris* were described using quantile-cantered trends. These involved the calculation of the median, the median absolute deviation (MAD), and the robust coefficient of variation (RCV). To identify multivariate outliers, a specialized *k*-nearest neighbours method based on the local outlier factor (KNN-LOF) was implemented [164]. This method utilized Minkowski distances, with an optimal number of neighbours ($k = 7$) determined according to the Gap statistic **(Figure SI-1, Figure SI-2)** [148]. These analyses were conducted using the *dplyr*, *tidyr*, *Rlof*, *NbClust*, *foreach*, and *doParallel* libraries, as well as the *do_knno* function from the *adamethods* package in R version 4.40 [126]. Additionally, the assumption of multivariate normality was evaluated and rejected using the Doornik-Hansen omnibus test, the Energy test, and the generalized Shapiro-Wilk test. These tests were performed using the *MVN* and *mvShapiroTest* libraries in R version 4.40, with a significance level of 95 %.

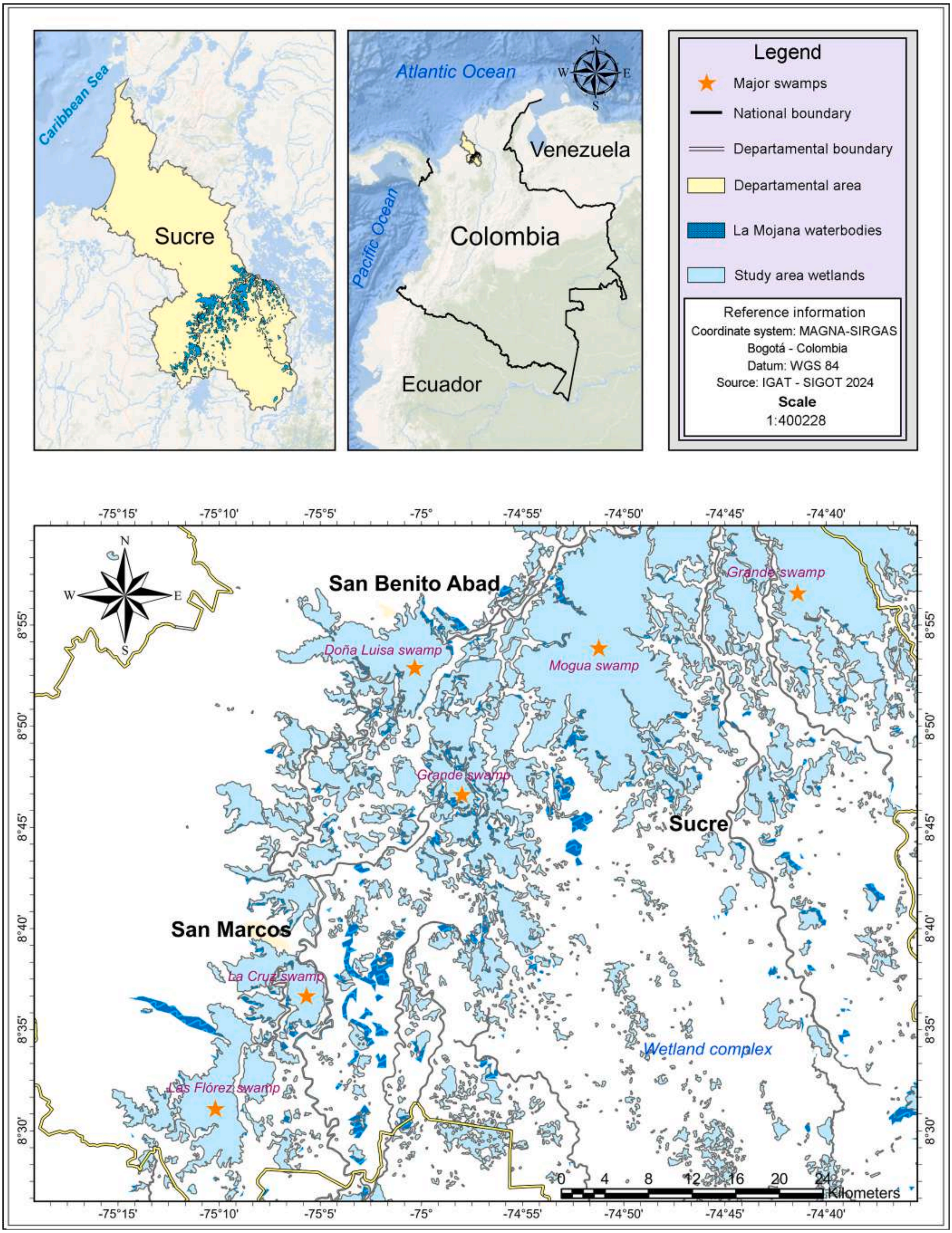

Fig. 1. Study area: location San Marcos, San Benito Abad and Sucre municipalities with their six major swamps in La Mojana region.

2.5.2. Differences between THg, MeHg, Pb, Cd, Cu, and Zn levels in muscle and liver

The analysis of differences in pollutants' concentrations between the two tissues was conducted using the robust Yuen-Welch test for dependent, non-normal, and heteroscedastic samples [158,159]. This test involved paired contrasts of the trimmed means (20 %) for each pollutant. A total of n = 10,000 bootstrap samples were generated to compute the explanatory measure of effect size (ξ) for the estimated differences in concentrations taking in account quantile divergences, representing a more robust generalization of Cohen's *d* [160]. The analyses were performed using the *yuend*, *Dqcomhd*, and *effsize* functions from the *WRS2* library [95] in R version 4.40, with a 95 % significance level.

2.5.3. Joint association between morphometry and pollutant accumulation patterns in muscle and liver

To evaluate the degree of correlation between the studied variables, we estimated Hoeffding's independency coefficient (D), based on the joint and marginal probabilities of association between variable pairs. This measure represents a more robust and informative index compared to Pearson, Spearman, and Kendall coefficients, as it accounts for monotonic, non-monotonic, and non-linear relationships, while assessing conditional dependencies among variables [61,73]. Due to the presence of detected outliers, the covariance matrix for correlation calculations was computed using Cauchy's robust density, eliminating potential biases arising from the influence of these points on the magnitude of the coefficients [57], since recorded Cu and Zn concentrations in both tissues were considerably higher than THg, MeHg, Cd and Pb concentrations; enabling a multivariate estimation which strongly penalizes matrix factorization solving possible estimation issues derived from such extremely high concentrations ranges [68]. These estimations were conducted using the *dplyr*, *tidyr*, *independence*, and *fitHeavyTail* libraries in R version 4.40, with a significance level of 95 %.

2.6. Co-occurrence of pollutant accumulation patterns with T. callirostris morphometry

2.6.1. Conditional partial correlations

In order to determine how weight, PL, and CL were multifactorially associate with the localized accumulation of THg, MeHg, Pb, Cd, Cu, and Zn in the muscle and liver of *T. callirostris*, an analysis using a Bayesian undirected graphical model (BUGM) was performed [153]. This model consisted of a network of conditional partial correlations derived from uncertainty estimation with a birth-death continuous sampler based on the Markov Chain Monte Carlo (MCMC) method (BDMCMC), implemented using the *BDgraph* library in R 4.40 [113]. The BDMCMC sampler is a generalization of the reversible jump sampler based on the Markov Chain Monte Carlo method (RJMCMC) [66] and represents a more efficient and precise method than other classical samplers (Metropolis-Hastings, Gibbs, etc.) in inferring plausible structures in undirected graphical models [112].

In this regard, we utilized the number and magnitude of Hoeffding coefficients that represented evidence of appreciable conditional dependencies (D > 0.20, $p < 0.05$) to perform the network structure learning. This was done by applying a restrictive prior on correlations' inclusion probabilities (edges), as well as an informative prior based on the current knowledge and certainty regarding the number and magnitude of probable dependencies (**Table SI-2**). It is important to note that using informative priors tends to generate more accurate and efficient inferences, while also significantly reducing the uncertainty threshold in the posterior distribution [172]. This is because informative priors control potential spurious and confounding events that introduce noise and biases into the sampling process [91], particularly in small sample sizes [143,171]. Additionally, a proper understanding and adjustment of priors in Bayesian inference applied to graphical structure learning [87], selection through Bayesian Model Averaging (BMA) [88], and the operational nature of conditional partial correlations graphical models [52,71] provide an effective framework for modelling complex relationships, even in the presence of multicollinearity.

Thus, the samplings were executed over 160,000 iterations, discarding 70,000 iterations in the burn-in phase (< 50 % of the total iterations, [77]). A G-Wishart distribution was used as the conjugate prior for the precision matrix, along with an inclusion probability of *g.prior* = 0.3, 7 degrees of freedom (*df.prior* = 7), and 10 jumps to control the autocorrelation rate between iteration lags and ensure independent and stable convergence towards the stationary behaviour of the posterior distribution. Consequently, the network was constructed as a Gaussian copula graphical model (GCGM) [111], due to the previously determined absence of multivariate normality. It is also necessary to note that, due to the sensitivity of the G-Wishart distribution to outliers, weight, PL and CL distributions and pollutants distributions in each tissue were individually recoded from their quantiles to eliminate the biasing impacts of these atypical values performing a robust inference, while simultaneously preserving their conditional properties [120]. This procedure was carried out in MATLAB R2024a (The MathWorks Inc, Natick, Massachusetts).

As a result, the conditional partial correlations (Θ) and the inferred structure of the network (*S*) were selected by implementing BMA, which performs a robust and weighted selection on plausible structure probabilities with the least degree of uncertainty to generate the posterior distribution [93]. Subsequently, we estimated the Bayes factor 10 (BF_{10}) to determine the degree of evidence in favour of edge inclusion (*null hypothesis*) and exclusion (*alternative hypothesis*) in the selected correlation structure from the BMA [140] (**Table SI-3**). To assess the uncertainty and stability in the estimated partial correlations we quantified the 95 % high-density intervals (HDI), the forementioned procedures were executed using the *easybgm* library [78]. As a convergence quality diagnostic, autocorrelation function (ACF) and partial autocorrelation function (PACF) were plotted (**Figure SI-3**), along with the general convergence diagnostic (CODA) (**Figure SI-4**). These diagnostics were developed in R 4.40 using the *BDgraph* library.

2.6.2. Structure of conditional association patterns

The selected conditional partial correlations ($BF_{10} > 10$) derived from the BUGM learning were used as the association criteria (weights) in a graph analysis conducted with the *igraph* library in R 4.40. This analysis involved the creation of a weighted and undirected network using the Davidson-Harel [40] algorithm as the projection layer, based on the metaheuristic optimization approach of simulated annealing, along with the Johnson algorithm to compute all pairs of shortest paths between weight, PL, CL, and the accumulation patterns of THg, MeHg, Pb, Cd, Cu, and Zn in the muscle and liver of *T. callirostris*, given the sparse nature of the network [82]. In this regard, specific centrality metrics: degree, betweenness, closeness, and eccentricity were calculated for each of the variables or nodes, along with general network metrics such as assortativity, density, diameter, centralization, heterogeneity, and average path length [119,157,162]. Additionally, structural communality or clustering patterns were determined by quantifying modularity using a multi-level optimization approach in accordance with graph theory, implementing the Louvain algorithm [20] and its extension, the Leiden algorithm [149]. Finally, we estimated the intra-cluster correlation coefficients for each of the communities or groups detected with both algorithms.

3. Results

3.1. Descriptive aspects of morphometry and pollutant accumulation in T. callirostris muscle and liver

Table 1 shows that the median weight of *T. callirostris* ranged from 680 – 1634 g, with over 1000 g being the most frequent, describing the highest relative variability in the morphometry. Similarly, the PL and CL

Table 1
Descriptive statistics of morphometric variables with muscular and hepatic THg, MeHg, Pb, Cd, Cu and Zn concentrations in *T. callirostris* (in bold the medians within the referenced TRV range).

Measure	Variable	Min	Median	Max	IQR	MAD	RCV
Morphometry	Weight (g)	680.00	1032.00	1634.00	366.00	126.00	0.18
	PL (cm)	17.40	19.80	23.80	4.00	1.40	0.10
	CL (cm)	18.60	22.50	26.50	4.10	2.00	0.13
Muscle accumulation (μg/kg)	THg	34.34	**157.47**	456.19	238.63	101.16	0.95
	MeHg	22.89	96.38	245.55	136.28	56.83	0.87
	Pb	3.40	37.30	128.20	43.00	14.80	0.59
	Cd	7.50	19.80	40.40	11.00	5.00	0.37
	Cu	1200	2550	11600	3200	1050	0.61
	Zn	113400	175100	289300	52900	22100	0.19
Liver accumulation (μg/kg)	THg	77.71	**331.78**	1432.19	795.11	216.78	0.97
	MeHg	37.72	144.77	412.72	170.20	76.15	0.78
	Pb	107.90	253.20	408.70	125.90	51.70	0.30
	Cd	50.80	189.50	742.70	459.85	115.20	0.90
	Cu	6100	24100	90200	25200	14200	0.87
	Zn	46000	83400	154900	46400	17500	0.31

presented point distribution ranges from 17.40 – 23.80 cm and from 18.60 – 26.50 cm, respectively, with PL being the most homogeneous morphometric parameter. Median concentrations of pollutants in muscle and liver indicated that, in general, Cd and MeHg showed the lowest accumulation rates in muscle tissue and liver tissue, respectively. In contrast, Zn consistently presented the highest median concentrations in both tissues, breaking the generalized pattern of inter-tissue accumulation, through which THg, MeHg, Pb, Cd, and Cu accumulated more in the liver. Furthermore, in muscle tissue, the RCV revealed that the median amounts of Zn presented the lowest relative variation in accumulation, while THg exhibited the most variable accumulation behaviour. Similarly, in the liver, Pb exhibited the most homogeneous accumulative among the pollutants, while THg proved to be the pollutant with the highest cumulative heterogeneity across both tissues. In this context, median THg concentrations bioaccumulated in muscular and hepatic tissues were contrasted against median THg levels in *Caretta caretta* red blood cells found as hematotoxic by Day et al. [42] which correspond to the 100 μg/kg – 350 μg/kg range, serving as reference toxicity range value (TRV) for our findings.

3.2. Differences in bioaccumulated THg, MeHg, Pb, Cd, Cu, and Zn concentrations in T. callirostris muscle and liver

Fig. 2 shows that paired comparisons with the Yuen-Welch test revealed significant differences ($p < 0.05$) between the accumulated concentrations of these pollutants, except for MeHg, which accumulated with a consistent similarity in both tissue matrices (Fig. 2**b**). In this regard, the effect size measure of the estimates indicates that the differences in the accumulated amounts of THg (Fig. 2**a**), Pb (Fig. 2**c**), Cd (Fig. 2**d**), Cu (Fig. 2**e**), and Zn (Fig. 2**f**) in the liver and muscle of *T. callirostris* are large following the descendent hierarchy: Cd > Zn > Pb > Cu > THg. It is important to mention the presence of multiple outliers in each pollutant distribution, with graphical representations of some concentrations of Cd and Cu being omitted due to the severely leptokurtic behaviour of their distributions in muscle tissue.

3.3. Joint conditional associations between morphometry and pollutant accumulation patterns in muscle and liver

Only 20 (19.47 %) of the 105 possible correlation pairs exhibited significant and appreciable conditional association degrees ($D > 0.20$, $p < 0.05$). In this context, it is relevant to highlight that all Hoeffding coefficients represented positive associations, with THg and MeHg, both in muscle and liver, exhibiting the most pronounced and diversified dependencies. Regarding morphometry, the mutual association between CL and PL, the weight of the turtles, and THg concentrations in muscle was particularly notable, as well as the dispersed associations of these three measures with THg, MeHg, and Cd accumulation in liver tissue. In general, the estimated dependencies showed low-moderate and moderate-high magnitudes (**Table SI-2**).

3.4. Network of conditional partial correlations

Inference with the BUGM, the subsequent selection performed through BMA, and the estimation of BF_{10} revealed that only 13 associations (12.38 % of the total) had conclusive probabilities and evidence in favour of their inclusion in the model (**Table SI-3**). Thus, Cu in muscle was excluded from the correlation network, as no conditional associations between its accumulation in this tissue and the other variables were detected (Fig. 4**b**). Furthermore, 92 edges or associations (87.62 % of the total) showed sufficient evidence for their exclusion (Fig. 4**a**), which, along with the high posterior probability of the selected conditional partial correlation structure (S) ($p = 0.654$), reflects the BUGM capability to capture, with a high degree of certainty, the true nature of these complex multifactorial associations in *T. callirostris*. In this regard, only 21 structures (from 4.056482×10^{31} possible structures) were visited by the algorithm, given the restrictive and informative characterization of the prior implemented, significantly impacting in the sampling efficiency and precision (**Table SI-3**).

In the **Figure SI-3a**, it can be seen that the algorithm visited networks with a number of edges ranging from 4 to 26, with the network structure with 14 edges being the most visited. Additionally, the BDMCMC sampling convergence indicates that samples autocorrelation based on the ACF, decreased and stabilized quickly around five lags, whereas the partial autocorrelation observed in the PACF reached this behaviour before four lags (**Figure SI-3b, c**). In this regard, the traces show a total of 9000 samples, in which the algorithm converges with a predominant posterior link probability, prior to edge selection using BMA and the evidence confirmatory step with BF_{10}. Under these conditions, the CODA shows that near 3100 samples, the inference process stabilizes and becomes independent, reaching the stationary behaviour characteristic of the posterior distribution (**Figure SI-4**).

Upon reviewing Fig. 3, it is evident that conditional partial correlations' (Θ) magnitude and their respective 95 % HDI confirm the findings from BMA selection and BF_{10} regarding the inferred associations certainty, as the intervals generally reflect a high consistency and stability due to their relatively low width, which gradually increases as the correlation strength decreases. Regarding morphometry, the correlation structure shows a pattern of associations in which the CL exhibited the most pronounced relationship with Zn accumulation in muscle, followed by the relationships established by weight and PL. On the other hand, Zn and THg in muscle and liver, Cu in liver, Cd in muscle, MeHg in both muscle and liver, and Pb in both muscle and liver showed, in general, strong, moderate, and moderate-low conditional associations,

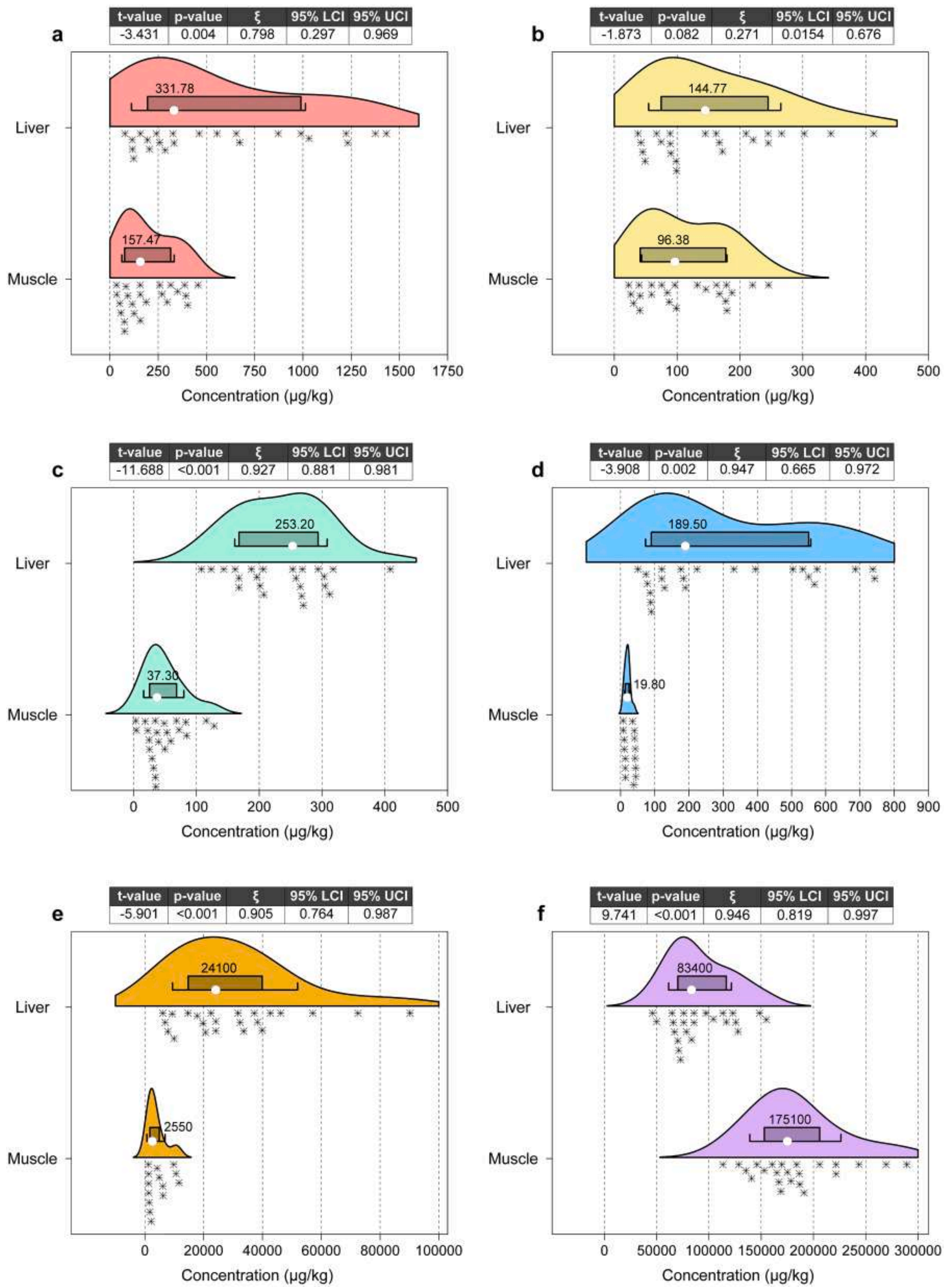

Fig. 2. Raincloud plots of THg (**a**), MeHg (**b**), Pb (**c**), Cd (**d**), Cu (**e**), and Zn (**f**) distributions and medians in muscle and liver. The t-values, probabilities, and ξ with their respective 95 % confidence intervals (CI) of estimated differences between the accumulated concentrations are shown.

respectively, being the relation between the CL and MeHg accumulative patterns in muscle the weakest, with all Θ describing a positive nature. It is important to highlight that Zn in muscle and liver, Cu in liver, Cd in muscle, and MeHg in muscle were the only five pollutants that exhibited conditional partial correlations with *T. callirostris* morphometry.

3.5. Structure of conditional association patterns

Table 2 reveals that the graph possesses a complex and highly centralized structure around certain variables. In this context, MeHg accumulation in muscle emerges as the most prominent node, with the

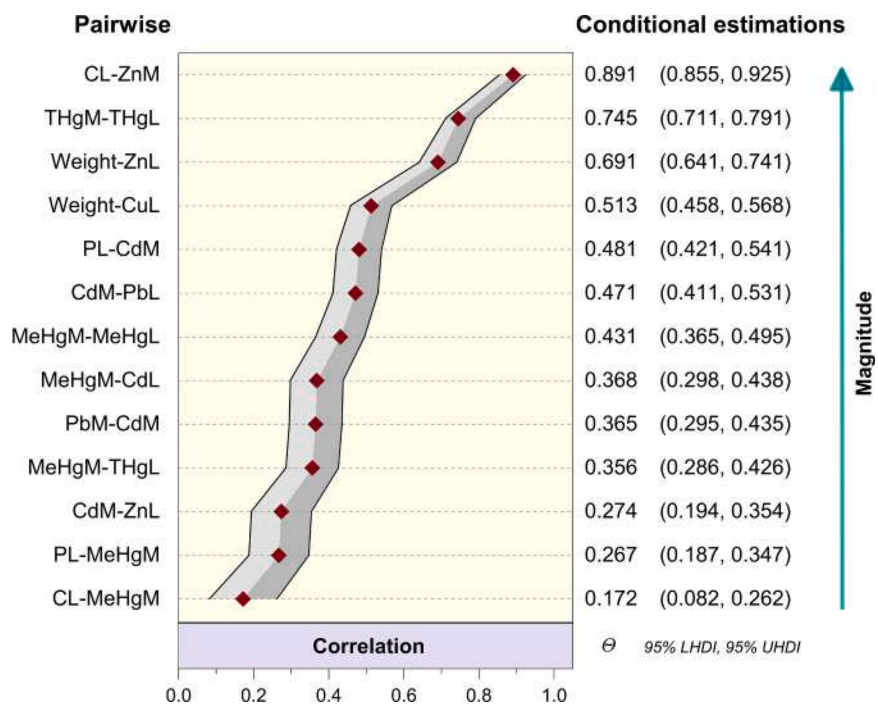

Fig. 3. Forest plot of conditional partial correlations (*Θ*) and their respective 95 % HDI in light grey (lower density interval) and dark grey (upper density interval).

Table 2
Centrality metrics of THg, MeHg, Pb, Cd, Cu, and Zn structural accumulation patterns in *T. callirostris*.

Variable	Degree	Betweenness	Closeness	Eccentricity
MeHg**M**	5	55	1.102	5
Cd**M**	4	47	1.019	4
PL	2	42	1.102	4
CL	2	12	0.962	6
Weight	2	12	0.595	6
THg**L**	2	12	0.847	6
Zn**L**	2	12	0.870	5
Pb**M**	1	0	0.759	5
THg**M**	1	0	0.535	7
Zn**M**	1	0	0.537	7
MeHg**L**	1	0	0.767	6
Pb**L**	1	0	0.706	5
Cd**L**	1	0	0.802	6
Cu**L**	1	0	0.464	7

*__M__= Muscle and **L** = Liver

highest degree of centrality and mediation, reflecting key associations in the accumulation patterns of MeHg, Cd, and THg in the liver, as well as its particular relationship with the turtles PL and CL, being the only pollutant associated with more than one morphometric parameter. In this sense, the high closeness degree of MeHg accumulation in muscle and its considerable eccentricity may suggest a systemic role in inter-tissue accumulation patterns of these pollutants, representing a bridge between local processes governing the accumulation of pollutants associated with changes in CL and PL, when considering all measured morphometric parameters influence in *T. callirostris*. In conjunction, Cd accumulation in muscle also plays a dominant role in these dynamics, as it directly associates with the accumulation of other trace elements, such as Pb in muscle and liver, as well as Zn accumulation in liver and PL, thus playing an integrative role in the structural bioaccumulation network (Fig. 4**c**). Playing a minor role in these dynamics, the accumulation of the closest pollutants linked to changes in turtles' weight.

On the other hand, the morphometry shows that PL and CL, although with a lower degree and intermediate centrality, are considerably integrated into the network, suggesting a relevant interaction with MeHg, THg, Cd, and Pb bioaccumulation patterns in muscle and liver, and Zn in muscle. In this regard, PL is the morphometric variable with the highest degree of closeness, reflecting a predominant influence on the structural proximity of various associations, while CL, with a slightly lower degree of closeness, exhibits a more eccentric and specialized role in the accumulation of these pollutants, especially Zn in muscle. The weight, with approximately half of the PL and CL closeness degree, shows a marked tendency to associate with Zn and Cu accumulation patterns in the liver (Fig. 4**c**). In contrast, the accumulation of Cu in the liver, Pb in muscle and liver, THg and Zn in muscle, Cd and MeHg in liver, shows low intermediate centrality, suggesting that their accumulation processes tend to be mainly peripheral and more restricted, with fewer direct associations in the structural accumulation dynamics. This is evidenced by the cumulative eccentricity of Cu in liver and THg and Zn in muscle, which would confirm their cumulative specificity under metabolic and physiological conditions that imply significant changes in the turtles' weight and CL (Table 2; Fig. 4**c**).

3.6. Co-occurrence of pollutant accumulation in muscle and liver with *T. callirostris* morphometry

In Table 3, the network' general characteristics indicate that it possesses a negative assortativity, which suggests that the association patterns between morphometry and THg, MeHg, Pb, Cd, Cu, and Zn accumulation exhibit a disassortative behaviour, a feature property of biological networks. This indicates that cumulative processes represented by the more central nodes, such as MeHg and Cd in muscle, tend to associate with changes in morphometric variables and the accumulation of pollutants that possess lower centrality degrees (Fig. 4**c**). Consequently, the network's low-density structure aligns with the observed disassortativity, as the number of associations between the nodes is scarce, with dispersed interactions between the cumulative processes of pollutants in muscle and liver and *T. callirostris* morphometry. Furthermore, the network diameter and its average path length suggest that, despite its low-density, the co-occurrence of the studied variables is structurally efficient, with changes in PL, CL, and weight playing a connecting role in the transport mechanisms and joint THg, MeHg, Pb, Cd, Cu, and Zn accumulation between the muscular and

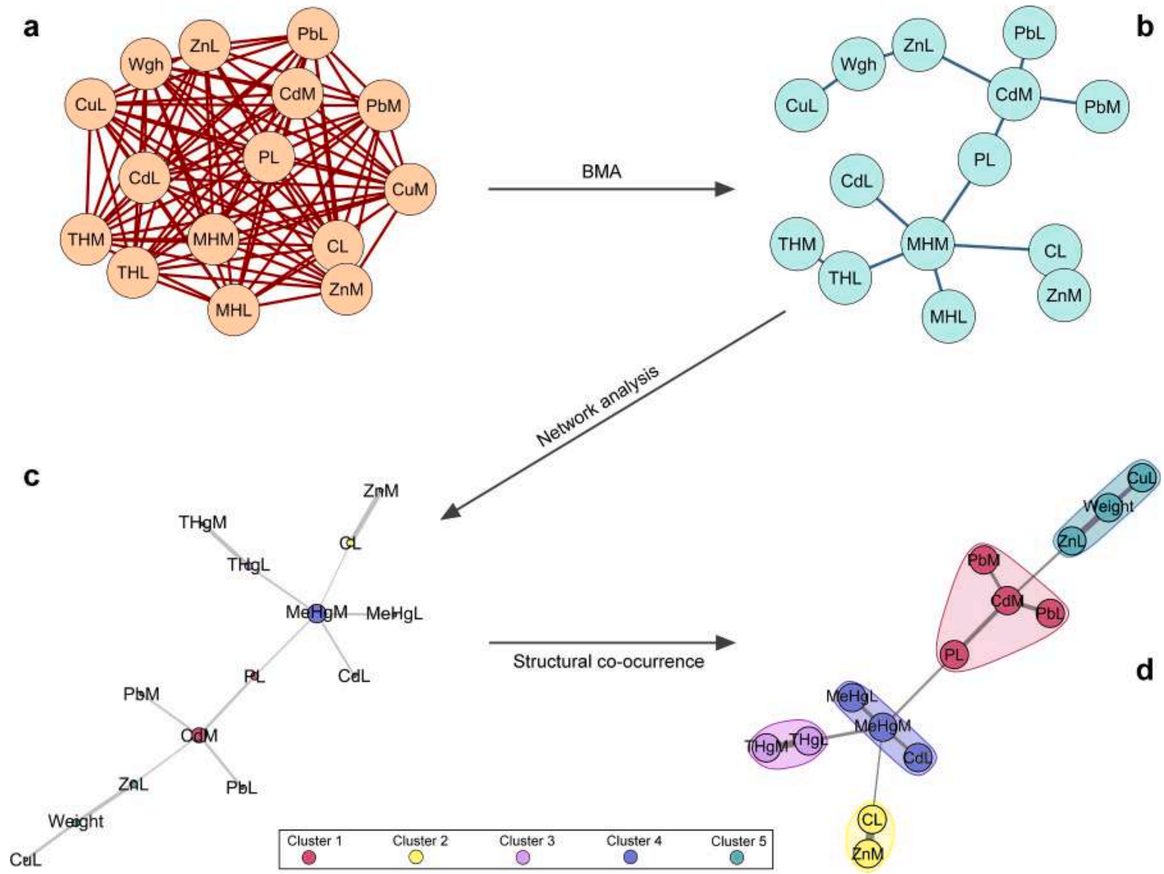

Fig. 4. Sequential assessment of conditional partial correlations (**a**, **b**) and the structural dynamics of co-occurrence between *T. callirostris* morphometry and THg, MeHg, Pb, Cd, Cu, and Zn accumulation in muscle and liver (**c**, **d**).

Table 3
General and modularity metrics in THg, MeHg, Pb, Cd, Cu, and Zn structural accumulation patterns in *T. callirostris* (in bold the best modularity and intra-cluster cohesion coefficients).

Metric	Value
Modularity through Louvain algorithm	0.614
Modularity through Leiden algorithm	**0.698**
Assortativity	−0.513
Density	0.143
Diameter	3.326
Centralization	0.242
Heterogeneity	0.663
Average path length	1.358
Size	14
Total edges	13
ICTLVA (Cluster 1)	0.220
ICTLVA (Cluster 2)	0.890
ICTLVA (Cluster 3)	0.745
ICTLVA (Cluster 4)	0.266
ICTLVA (Cluster 5)	0.401
ICTLDA (Cluster 1)	**0.231**
ICTLDA (Cluster 2)	**0.913**
ICTLDA (Cluster 3)	**0.782**
ICTLDA (Cluster 4)	**0.275**
ICTLDA (Cluster 5)	**0.424**

hepatic tissues.

The network centralization patterns and its high heterogeneity show that it is relatively centralized, with a notable variation in node connectivity. This is consistent with the finding that MeHg and Cd accumulation in muscle, which were conditionally associated with variations in PL, CL, and weight, may play more generalized and structurally relevant roles in co-occurrence dynamics. In contrast, other nodes, such as Zn and THg accumulation in muscle, and Cu in liver, may be restricted to highly specific co-occurrence conditions or influenced by particular environmental or physiological factors (Table 2**;** Table 3).

The modularity (intra-cluster cohesion) calculated through the Louvain (ICTLVA) and Leiden (ICTLDA) algorithms reveals that, topologically, network stratification is high and consistent, implying that pollutants accumulation in muscle and liver, along with the PL, CL, and weight, co-occur in defined groupings, within which the nodes are more densely and strongly connected to each other than to nodes from other communities. In this regard, the ICTLDA detected the modularity of these associations more efficiently than the ICTLVA, although the differences between both clustering coefficients were not high. Consequently, the intra-cluster cohesion detected by the ICTLVA was also lower than the intra-cluster cohesion detected by the ICTLDA in each of the five clusters or differentiated communities in the network (Table 3).

Based on these findings, cluster 1 grouped the PL, Pb and Cd accumulation in muscle, as well as Pb accumulation in the liver, with low-moderate intra-cluster cohesion, suggesting heterogeneous co-occurrence patterns between the accumulation rates of these pollutants and possible general changes in the PL of *T. callirostris*. In contrast, cluster 2 exhibited the highest degree of cohesion, involving the relationship between changes in the CL and Zn accumulation in muscle, pointing towards potential shared physiological mechanisms of co-occurrence. Meanwhile, cluster 3 was exclusively structured by THg accumulation in muscle and liver, showing high intra-cluster cohesion, which would reinforce evidence of shared distribution and accumulation dynamics of this mercurial species between both organic matrices. Cluster 4, consisting of MeHg accumulation in muscle with MeHg and Cd accumulation in liver, presented a low-moderate degree of cohesion, describing less pronounced interactions between this bioactive mercury form and Cd accumulation patterns, which could be anchored to cumulative changes in turtles' muscular tissue. In this context, cluster 5, with moderate cohesion, encompasses the associations between weight and Cu and Zn accumulation in liver, indicating a direct influence of weight changes on these elements accumulation rates into the hepatic matrix (Fig. 4**d**).

4. Discussion

4.1. Descriptive bioaccumulation in liver and muscle

The results revealed clear patterns of differential pollutant accumulation in *T. callirostris*, with most elements (THg, Pb, Cd, and Cu) showing higher concentrations in the liver, consistent with its central role in detoxification and metal sequestration via metallothioneins, glutathione, and other complexes, as well as in biotransformation into less toxic forms [110,167,5,7,70]. This hepatic predominance is widely documented in turtles from diverse aquatic systems [67,41,45,65,124]. In contrast, Zn showed high concentrations in both tissues, but significantly higher in muscle, likely due to its essential role in contraction, enzymatic regulation, cellular homeostasis, and structural integration into myofibrillar proteins [29,146,90]. Elevated hepatic Zn may also relate to its participation in detoxification and oxidative stress mitigation via metallothioneins [13,155,35], consistent with previous findings in *C. caretta* and *Phrynops geoffroanus* [56,94].

Comparison with other studies showed both similarities and differences in metal concentrations across species and sites (**Table SI-4**) Hepatic THg levels (331.8 μg/kg) exceeded those previously reported for the same species in La Mojana [110] and for *P. unifilis* in the Amazon [124], although remained below the values observed in *C. caretta* [41] and *T. scripta elegans* [167]. THg concentrations in muscle were lower than those previously reported for *T. callirostris* by Zapata et al. [168] in a region adjacent to La Mojana, within the San Jorge basin, but higher than in *P. unifilis* [124]. Moreover, although Rendón-Valencia et al. [128] did not assess internal tissues, they reported mean THg levels of 31 μg/kg in yolks and 79 μg/kg in embryos of *T. callirostris*, evidencing maternal Hg transfer and regional exposure. MeHg levels in both liver and muscle were similar to those reported for *C. mydas* [165], suggesting a comparable bioaccumulation pattern. For Pb, liver concentrations in *T. callirostris* were slightly higher than in *T. scripta* [167], while muscle levels were strongly lower [167]. Cd levels in both tissues were consistently lower than those recorded under dietary exposure in *T. scripta* [70]. Cu accumulation in liver was similar to *C. mydas* [45], higher than *T. scripta* [167], and lower than *C. caretta* [94], with muscle values also below those observed in *T. scripta* [167]. Muscle Zn concentrations were very high, aligning with the levels reported in *C. caretta* [94], reflecting significant exposure to this essential element.

The observed variability may be related to seasonality, trophic exposure, food availability, and life stage. Sampling was conducted during the rainy season in La Mojana, when intense precipitation and flooding (>500 mm/month in some areas; **Table SI-5**) enhance wetland connectivity and promote pollutant mobilization through surface runoff and sediment resuspension ([80]). Under these conditions, *T. callirostris* may be exposed to both diffuse and point sources of pollution via ingestion of benthic invertebrates, fish, or aquatic vegetation ([104]; Urango-Cárdenas et al., 2024; [79]). Only similarly sized adult individuals were included, based on the availability of specimens provided by authorized local fishers, which limits extrapolation to juveniles or reproductive stages that may exhibit different bioaccumulation dynamics [108,30]. Furthermore, turtles were collected from wetlands influenced by the San Jorge, Magdalena, and Cauca rivers, three basins with distinct pollutant profiles, including ASGM in San Jorge ([98]; 2021), agricultural runoff and urban effluents in Magdalena [31], and mixed industrial-agricultural pressures in Cauca [104]. These basin-level contrasts likely contribute to the observed accumulation patterns and underscore the importance of spatially explicit biomonitoring strategies [18,92].

In particular, the high THg variability, especially in muscle, may reflect irregular exposure linked to ASGM in the upper Cauca and San Jorge basins, whose waters reach La Mojana [98]. In contrast, liver Pb showed more consistent accumulation, possibly from historical pesticide and fertilizer residues and diffuse runoff from crops like rice [98,100,101,89]. This is consistent with *M. leprosa* in Spain, where Hg and Pb bioaccumulation was associated with historical mining [117]. Hepatic Pb storage may also be linked to hematopoietic activity and iron storage roles of the liver [127,31].

4.2. Significant inter-tissue differences

Robust statistical analyses (Yuen-Welch test) confirmed significant inter-tissue differences for all metals except MeHg, whose homogeneous distribution reinforces its systemic nature. MeHg exhibits high bioavailability, cellular permeability via methionine mimicry, and strong affinity for sulfhydryl groups in muscle proteins and keratin [110,38,70]. In muscle, MeHg binds stably to structural proteins, while in liver it undergoes partial enzymatic demethylation and sequestration via glutathione pathways [5,7], explaining the observed symmetry and its correlation with hepatic THg [5,7,70].

The inter-tissue effect size hierarchy (Cd > Zn > Pb > Cu > THg) suggests physiological prioritization in metal processing. Cd showed the greatest contrast, consistent with its hepatotoxicity and affinity for intracellular detoxification [167,56,70,94]. Zn, though essential, accumulated highly in both tissues, reflecting both physiological storage and environmental exposure ([35]; ; [89]). This duality has ecotoxicological implications, particularly in La Mojana, where turtles are consumed by humans [98], potentially modulating health risks depending on tissue-specific pollutant retention.

4.3. Associations between morphometry and pollutant accumulation in liver and muscle

Conditional partial correlation analysis revealed that only a small subset of associations showed conclusive evidence, indicating a highly structured bioaccumulation network in *T. callirostris*. Among these, morphometric variables such as CL, PL, and weight were particularly relevant, especially their associations with Zn and Cu [138,167,97]. The strongest associations were between CL and Zn in muscle, followed by weight with Zn and Cu in liver, supporting the role of body size in the accumulation of essential elements due to increased storage capacity, exposure time, and ontogenetic changes in physiology or diet [141,29,58,62]. PL also correlated with Cd and MeHg in muscle, suggesting cumulative exposure to persistent pollutants [141,29].

It is important to note that only Zn, Cu, Cd, and MeHg showed conditional associations with morphometry. Pb and THg correlated mainly among themselves or with their tissue-specific counterparts (e.g., MeHg–THg, PbM–CdM), likely reflecting co-storage or chemical relatedness [167,36]. Zn had the strongest size-dependent pattern (CL and weight), consistent with its known behaviour in aquatic organisms and dual role as essential element and marker of cross-pollution [56,94]. Its co-occurrence with Cu and Cd may stem from shared intracellular pathways [94].

THg showed moderate correlation between liver and muscle, but no morphometric link, suggesting systemic distribution and hepatic demethylation [124,41]. The association of Cu with weight in liver may indicate chronic exposure and sublethal effects on metabolism [138,58]. Cd in muscle correlated with PL and PbL, pointing to size-dependent accumulation and possible synergistic interaction [138,29]. MeHg showed inter-tissue and intra-tissue links (MeHgM–MeHgL, CdL, THgL), with weaker morphometric associations but signs of progressive bioaccumulation ([83]; Green et al., 2010; [45,81]). Pb had the weakest morphometric associations, but persistent correlations with Cd, possibly reflecting diffuse, long-term exposure [138,58,7]. These patterns reveal that bioaccumulation in *T. callirostris* follows a non-random structure, where key pollutants and morphometric traits (CL, PL) act as network hubs, while others remain peripheral. The low percentage of conclusive associations (12.38 %) further highlights the selective, functionally organized nature of this bioaccumulation network.

4.4. Structure and centrality in accumulation patterns

Bayesian conditional network analysis revealed MeHg in muscle as the most central node, with the highest degree, betweenness, and closeness centrality [11,27,51]. Its prominence underscores a systemic role in bioaccumulation across tissues, supported by associations with Cd and THg in liver and strong links to key morphometric traits (CL and PL) [165,81]. This dual functionality positions MeHgM as a biochemical bridge between tissue-specific accumulation and overall organismal condition. Similar patterns have been reported in marine turtles like *C. mydas* and *C. caretta*, where MeHg accumulates predominantly in muscle and correlates with CL [165,83].

Furthermore, Cd in muscle also exhibited high centrality, connected to Pb (both tissues), ZnL, and PL. This suggests involvement in multifactorial accumulation, potentially driven by co-regulation mechanisms or shared environmental pressures [29,70,85]. The central topological positions of MeHg and Cd likely arise from a combination of ecological and environmental factors [15,55]. Both metals may enter the food web through common dietary routes (e.g., benthic invertebrates and small fish), and are also among the most widespread pollutants in La Mojana due to upstream ASGM (MeHg) and agricultural activities (Cd) [102,60]. Their systemic distribution and persistence further contribute to their network prominence [104]. Yet, as the BUGM model captures conditional dependencies rather than directionality, confirming causal pathways would require additional evidence (e.g., dietary profiles) [96,140].

Morphometric traits such as PL and CL showed moderate centrality, influencing network structure despite their intermediate degree values. PL, with the highest closeness, functioned as a connector, while CL linked mainly to ZnM, consistent with studies showing metal accumulation in carapace and plastron as indicators of environmental exposure [138,33,58,97]. In contrast, weight showed limited connectivity, mainly associating with Cu and Zn in liver, pointing to a more localized hepatic role [138,33]. Peripheral nodes such as CuL, Pb, THg, and ZnM had low centrality, likely due to sporadic exposure or compartmentalized physiological roles [5]. While some associations reflect functional links (e.g., Zn–Cu–Cd via shared detox pathways), others may result from coincidental co-exposure (e.g., Pb–Cd from runoff), or chemical affinity (e.g., MeHg–THg interconversion) [167,36].

Global network metrics support a compact and interconnected structure: a small diameter (3.33) and short average path length (1.36) suggest that most variables are separated by only one or two steps. This indicates a high degree of integration among metals and morphometry, where perturbations (e.g., increased pollutant exposure) could affect the network broadly and quickly [96,140]. Hence, central pollutants like MeHg and Cd may function as keystone variables, relevant for both biomonitoring and mitigation.

4.5. Structural modulation and functional co-occurrence

The modularity-based analysis revealed a non-random organization of associations, structured into five functional clusters. Cluster 2 (CL–ZnM) showed the highest internal cohesion, highlighting the link between body size and Zn accumulation in muscle. Cluster 3 (THgM–THgL) confirmed a shared distribution of total mercury between tissues. Clusters 1 (CdM, PL, PbM, PbL) and 4 (MeHgM, MeHgL, CdL) revealed structural interactions between morphometry and toxic metals, while Cluster 5 (weight, CuL, ZnL) pointed to hepatic accumulation influenced by body size. The negative assortativity, the heterogeneity, along with the low-density and moderate diameter of the network, suggests that the biggest and most central nodes such as MeHgM or CdM tend to connect with smallest and most peripheral ones, being in agreement with ubiquitous patterns observed in biological networks, implying the high network modularity and its community differentiation might be product of specialized homeostatic mechanisms that controls turtles' organism responses to heavy metal bioaccumulation [11,136,27,51].

These patterns suggest functionally differentiated co-occurrence between morphometry, tissue accumulation, and pollutant chemistry, likely shaped by endogenous physiology, seasonal pollution, and local waterbody conditions [12,137,156,17,4]. Notably, Zn reached extreme concentrations in muscle (up to 175,100 μg/kg), raising concern despite its essentiality, as similar levels have been associated with adverse effects in other taxa [53]. MeHg emerged as the most central and integrative element, supporting its role in biomagnification, as observed in other Amazonian reptiles [36]. As well, median THg concentrations in muscle and liver (157.47 μg/kg and 331.78 μg/kg) were within the observed hematotoxicity range in red blood cells (100 μg/kg - 350 μg/kg) of *C. caretta* [42], and above the general 100 μg/kg toxicity threshold suggested as safe for wild fauna [54] leading to potential adverse effects on condition, reproduction and embryonic survival [74]. In this way, given their susceptibility to metal(loid) bioaccumulation, chelonians like *T. callirostris* may serve as effective bioindicators of polluted environments [145].

Furthermore, THg concentrations in liver surpassed the 200 μg/kg threshold set by WHO for fish consumption in vulnerable human groups (children under 15 years and childbearing women) [161], raising public health concerns [46]. Similarly, hepatic Cd and Pb accumulation near or above 200 μg/kg may pose chronic toxicological risks to La Mojana communities, who depend on this species for protein, while also threatening its ecological stability [14]. These findings call for urgent action to reduce pollutant inputs [121,170], protect sentinel and vulnerable species like *T. callirostris* [145,168], and ensure food safety in vulnerable wetland-dependent communities [22]. In this regard, a combination of ecotoxicological monitoring, source control, and community-based management program is required to mitigate long-term risks in La Mojana [6].

4.6. Study Limitations

Although the BUGM approach is robust for identifying structural dependencies even with small sample sizes, it infers statistical associations rather than causality. While morphometric traits such as PL and weight were conditionally associated with specific pollutants, these relationships should not be interpreted as direct effects. The absence of ecological covariates (e.g., diet, sex, age) and the potential heteroscedasticity in essential metal concentrations (e.g., Zn, Cu) may also limit generalisation. Moreover, *T. callirostris* were collected only from six marshes within La Mojana during a single season, which does not capture spatiotemporal aspect, i.e., seasonal and habitat variability or broader spatial heterogeneity. No measurements were made of water, sediment or prey items in parallel therefore the exposure pathways and source attribution could not be pinpointed for primary pollutant sources. Destructive sampling, i.e., the sacrifice of *T. callirostris*, was required to obtain the samples of muscle and liver, restricting sample size and precluding longitudinal monitoring. Future research should employ non-invasive sampling protocols, e.g., blood draws, keratinous scute clipping, especially when working with endangered species such as *T. callirostris*. Furthermore, the present study focused on pollutant concentrations, without measuring biomarkers of oxidative stress, detoxification enzymes or endocrine disruption thus omitting the potential of physiological impact. Despite these constraints, the present study represents a significant advance by applying a Bayesian network approach to evaluate multimetallic bioaccumulation patterns in *T. callirostris*, providing a robust foundation for subsequent investigations. By incorporating non-invasive sampling, ecological covariates and temporal dynamics into the BUGM framework, future work can not only address these limitations but also deepen our mechanistic understanding of pollutant bioaccumulation in *T. callirostris*, ultimately enhancing its value as a bioindicator for wetland health.

5. Conclusions

This study reveals structured, tissue-specific patterns of heavy metal accumulation in *Trachemys callirostris*, highlighting liver as the primary site for most pollutants, while Zn accumulates preferentially in muscle and shows strong positive associations with body size. MeHg exhibited the highest network centrality and homogeneous distribution across tissues, acting as a key integrative pollutant connected to PL, CL, and other toxic elements such as Cd and THg in liver. Cd in muscle also showed high centrality and strong links to PL, suggesting multifactorial accumulation influenced by both morphometry and environmental exposure. The BUGM enabled identification of conditional associations with high statistical support, uncovering five modular clusters in which morphometric traits co-occurred with specific metal groups. Zn and MeHg emerged as pivotal nodes, with Zn linked to CL and muscle-specific accumulation, and MeHg bridging multiple pollutants and morphometric traits. The network's negative assortativity may reflect coordinated systemic responses to multimetallic exposure. These results establish a novel probabilistic framework to understand pollutant–morphometry interactions in highly polluted freshwater ecosystems. *T. callirostris* is reaffirmed as a promising bioindicator for environmental monitoring. Future studies should integrate variables such as age, diet, and exposure history to refine mechanistic interpretations of these bioaccumulation patterns.

Environmental Implication

Morphometric traits, particularly plastron length changes, critically influence multimetallic bioaccumulation dynamics in *Trachemys callirostris*, establishing a mechanistic link between organismal biology and bioaccumulation in highly polluted aquatic ecosystems. Methylmercury (MeHg) and cadmium (Cd) identification as central nodes in a modular disassortative network, reveals their systemic integration with growth-related morphometrics, suggesting that developmental constraints or adaptive trade-offs could govern pollutants uptake. These findings extend conventional single-metal biomonitoring approaches, advocating for trait-based models to capture eco-physiological complexity. Detection of Total mercury (THg) concentrations in muscle and liver within hematotoxic thresholds in chelonians, further highlights potential public health and conservation risks.

CRediT authorship contribution statement

Jorge Bernal-Alviz: Writing – review & editing, Writing – original draft, Visualization, Validation, Software, Methodology, Formal analysis, Data curation, Conceptualization. **Tapia-Contreras Eunice:** Investigation. **Atri Seña-Gaibao:** Investigation. **Jorge Buelvas-Soto:** Writing – review & editing, Writing – original draft, Methodology. **José Marrugo-Negrete:** Writing – review & editing, Supervision, Resources, Methodology, Funding acquisition. **Moyano-Salcedo Álvaro:** Writing – review & editing, Writing – original draft, Methodology. **Dora Bjedov:** Writing – review & editing, Writing – original draft, Methodology, Conceptualization. **Leonomir Córdoba-Tovar:** Writing – review & editing, Writing – original draft, Methodology.

Declaration of Competing Interest

Authors declare no conflicts.

Acknowledgements

The authors are grateful to the members of the Laboratory of Toxicology and Environmental Management of the University of Córdoba (Colombia) and the University of Córdoba through the FCB-02–17 project for funding this research. This study was funded by CYTED (Programa Iberoamericano de Ciencia y Tecnología para el Desarrollo), through the Red MERCURED (420RT0007).

Appendix A. Supporting information

Supplementary data associated with this article can be found in the online version at doi:10.1016/j.jhazmat.2025.139487.

Data availability

Data will be made available on request.

References

[1] Adamovicz, L., Griffioen, J., Cerreta, A., Lewbart, G.A., Allender, M.C., 2019. Tissue enzyme activities in free-living eastern box turtles (terrapene carolina carolina). J Zoo Wildl Med 50 (1), 45–54. https://doi.org/10.1638/2018-0079.

[2] Agudelo-Echavarría, D.M., Olid, C., Molina-Pérez, F., Vallejo-Toro, P.P., Garcia-Orellana, J., 2020. Historical reconstruction of Small-scale gold mining activities in tropical wetland sediments in bajo Cauca-Antioquia, Colombia. In: In Chemosphere, 254. Elsevier BV, 126733. https://doi.org/10.1016/j.chemosphere.2020.126733.

[3] Aguilera-Díaz, M.M., 2004. La mojana: riqueza natural y potencial económico. Banco De la República. https://doi.org/10.32468/dtseru.48.

[4] Ali, H., Khan, E., 2018. Trophic transfer, bioaccumulation, and biomagnification of non-essential hazardous heavy metals and metalloids in food chains/webs—Concepts and implications for wildlife and human health. In: Human and Ecological Risk Assessment: An International Journal, 25. Informa UK Limited, pp. 1353–1376. https://doi.org/10.1080/10807039.2018.1469398.

[5] Ali, Z., Khan, I., Iqbal, M.S., Zhang, Q., Ai, X., Shi, H., Ding, L., Hong, M., 2023. Toxicological effects of copper on bioaccumulation and mRNA expression of antioxidant, immune, and apoptosis-related genes in Chinese striped-necked turtle (*mauremys sinensis*). In: In Frontiers in Physiology, 14. Frontiers Media SA. https://doi.org/10.3389/fphys.2023.1296259.

[6] Amini, Z., Hatami-Manesh, M., Aazami, J., Savabieasfahani, M., 2024. Ecological risk assessment of heavy metals (Pb, Cd, Cr, Ni, Zn, Fe) and metalloid (As) in surface sediment of anzali international wetland, Iran. Geol Ecol Landsc 1–19. https://doi.org/10.1080/24749508.2024.2373488.

[7] Andreani, G., Santoro, M., Cottignoli, S., Fabbri, M., Carpenè, E., Isani, G., 2008. Metal distribution and metallothionein in loggerhead (Caretta caretta) and Green (*chelonia mydas*) sea turtles. In: In Science of the Total Environment, 390. Elsevier, pp. 287–294. https://doi.org/10.1016/j.scitotenv.2007.09.014.

[8] Arenas, A.A., Di Luccio, D., Palmisano, S.M.M., Arévalo, L.S., Sanguino, R.A.M., & Lay-Ekuakille, A. (2022). Geochemical characterization of heavy metals in the sediments of the Sinú river (Colombia). 9th EnvIMEKO Symposium of Environmental Instrumentation and Measurements. June 2-3, 2022, Le Mans, France. 〈https://www.imeko.org/index.php/proceedings/9153-geochemical-characterization-of-heavy-metals-in-the-sediments-of-the-sinu-river-colombia〉.

[9] Arias, J.C.L., 2018. Plantas de los humedales de la mojana, Colombia [Dataset. Inst De InvestóN De Recur Biológicos Alexander Von Humboldt. https://doi.org/10.15472/EYFMEV.

[10] Arias, J.C.L., 2018. Vertebrados de los humedales de la mojana, Colombia [Dataset. Inst De InvestóN De Recur Biológicos Alexander Von Humboldt. https://doi.org/10.15472/E7EZBX.

[11] Ayre, K.K., Landis, W.G., 2012. A Bayesian approach to landscape ecological risk assessment applied to the upper grande ronde watershed, oregon. Hum Ecol Risk Assess 18 (5), 946–970. https://doi.org/10.1080/10807039.2012.707925.

[12] Bae, J.H., Lim, S.Y., 2012. Effect of season on heavy metal contents and chemical compositions of chub mackerel (*scomber japonicus*) muscle. In: In Journal of Food Science, 77. Wiley. https://doi.org/10.1111/j.1750-3841.2011.02530.x.

[13] Baird, S.K., Kurz, T., Brunk, U.T., 2006. Metallothionein protects against oxidative stress-induced lysosomal destabilization. Biochem J 394 (1), 275–283. https://doi.org/10.1042/BJ20051143.

[14] Barrios-Santana, Y.J., Mendoza-Benavides, S., Sampedro-Marín, A.C., Vergara-Mercado, M.C., 2021. Consumo y comercio de tortugas continentales en la subregión la mojana, Sucre, Colombia. In Revista de la Asociación Colombiana de Ciencias Biológicas. Asociacion Colombiana de Ciencias Biologicas, pp. 83–93. https://doi.org/10.47499/revistaaccb.v1i33.238.

[15] Becker, D.N., Brown, D.J., Hubbart, J.A., Anderson, J.T., 2025. Environmental factors influencing bioaccumulation of xenobiotic metals in freshwater turtles. Environ Pollut Bioavailab 37 (1), 2474007. https://doi.org/10.1080/26395940.2025.2474007.

[16] Bergeron, C.M., Husak, J.F., Unrine, J.M., Romanek, C.S., Hopkins, W.A., 2007. Influence of feeding ecology on blood Mercury concentrations in four species of turtles. In: In Environmental Toxicology and Chemistry, 26. Wiley, pp. 1733–1741. https://doi.org/10.1897/06-594r.1.

[17] Bernal-Alviz, J., Córdoba-Tovar, L., Pastrana-Durango, D., Molina-Polo, C., Buelvas-Soto, J., Cruz-Esquivel, Á., Marrugo-Negrete, J., Díez, S., 2025. Influence

of environmental and biological factors on Mercury accumulation in fish from the atrato river basin, Colombia. In: In Environmental Pollution, 366. Elsevier BV, 125345. https://doi.org/10.1016/j.envpol.2024.125345.
[18] Bessa, A.Z.E., 2023. Spatial variation, ecological risk, and point sources of environmental trace metals in lacustrine ecosystems: an assessment of natural and urban inputs. Soil Sediment Contam Int J 33 (7), 1062–1086. https://doi.org/10.1080/15320383.2023.2293866.
[19] Bjedov, D., Bernal-Alviz, J., Buelvas-Soto, J.A., Jurman, L.A., Marrugo-Negrete, J. L., 2024. Elevated heavy Metal(loid) blood and feather concentrations in wetland birds from different trophic levels indicate exposure to environmental pollutants. In: In Archives of Environmental Pollution and Toxicology, 87. Springer Science and Business Media LLC, pp. 127–143. https://doi.org/10.1007/s00244-024-01085-7.
[20] Blondel, V.D., Guillaume, J.-L., Lambiotte, R., Lefebvre, E., 2008. Fast unfolding of communities in large networks. In: In Journal of Statistical Mechanics: Theory and Experiment, 2008. IOP Publishing, p. P10008. https://doi.org/10.1088/1742-5468/2008/10/p10008.
[21] Bock, B.C., Páez, V.P., Cortés-Duque, J., 2015. Trachemys callirostris (Gray 1856). In: Morales-Betancourt, M.A., Lasso, C.A., Páez, V.P., Bock, B.C. (Eds.), Libro Rojo de Reptiles de Colombia. Instituto de Recursos Biológicos Alexander von Humboldt, Bogotá, Colombia, pp. 174–179. ⟨http://catalogo.humboldt.org.co/cgi-bin/koha/opac-detail.pl?biblionumber=18728⟩.
[22] Buelvas-Soto, J., Marrugo-Madrid, S., Marrugo-Negrete, J., 2021. Mercury and lead bioaccumulation in the *dendrocygna autumnalis* duck in the subregion of la mojana, Colombia. J MVZ Córdoba 26 (3), e2140. https://doi.org/10.21897/rmvz.2140.
[23] Burger, J., 1998. Effects of lead on behavior, growth, and survival of hatchling slider turtles. In: In Journal of Toxicology and Environmental Health, Part A, 55. Informa UK Limited, pp. 495–502. https://doi.org/10.1080/009841098158296.
[24] Burgos-Núñez, S., Navarro-Frómeta, A., Marrugo-Negrete, J., Enamorado-Montes, G., Urango-Cárdenas, I., 2017. Polycyclic aromatic hydrocarbons and heavy metals in the cispata bay, Colombia: a marine tropical ecosystem. In: In Marine Pollution Bulletin, 120. Elsevier BV, pp. 379–386. https://doi.org/10.1016/j.marpolbul.2017.05.016.
[25] Caraballo, P., De La Ossa V, J., 2011. Inundaciones en la mojana: ¿Vía crucis social o condición ambiental? Rev Colomb De Cienc Anim RECIA 3 (1), 198–210. https://doi.org/10.24188/recia.v3.n1.2011.362.
[26] Carrasco, L., Díez, S., Bayona, J.M., 2007. Methylmercury determination in biota by solid-phase microextraction. Journal of Chromatography A 1174 (1–2), 2–6. https://doi.org/10.1016/j.chroma.2007.09.051.
[27] Carriger, J.F., Parker, R.A., 2021. Conceptual Bayesian networks for contaminated site ecological risk assessment and remediation support. J Environ Manag 278. https://doi.org/10.1016/j.jenvman.2020.111478.
[28] Castaño-Mora, O.V., 1997. Status of the tortoises and freshwater turtles of Colombia. In: Van Abemma, J. (Ed.), Proceedings: Conservation, Restoration, and Management of Tortoises and Turtles—An International Conference. New York Turtle and Tortoise Society, New York, pp. 302–306. In: ⟨https://www.nytts.org/proceedings/index.html⟩.
[29] Caurant, F., Bustamante, P., Bordes, M., Miramand, P., 1999. Bioaccumulation of cadmium, copper, and zinc in some tissues of three species of marine turtles stranded along the French atlantic coasts. In: In Marine Pollution Bulletin, 38. Elsevier Science Ltd, pp. 1085–1091. https://doi.org/10.1016/S0025-326X(99)00109-5.
[30] Çelik, S., Beton, D., Çiçek, B.A., Snape, R.T.E., Başkale, E., 2023. Metal accumulation in juvenile and sub-adult loggerhead and Green turtles in Northern Cyprus. Environ Pollut 316, 120482. https://doi.org/10.1016/j.envpol.2022.120482.
[31] Conrado, A.L.V., De Oliveira, A.C.P., Dos Santos Medeiros, L., Da Silva, T.L., De Carvalho, Y.K., 2023. Iron deposition in the liver and guts of giant south American freshwater turtle *podocnemis expansa* (Schweigger 1812) from a commercial breeding farm in acre, Brazil. Multidiscip Sci J 4 (4). https://doi.org/10.31893/multiscience.2022020.
[32] Córdoba-Tovar, L., Marrugo-Negrete, J., Ramos Barón, P.A., Calao-Ramos, C.R., Díez, S., 2023. Toxic metal(loids) levels in the aquatic environment and nuclear alterations in fish in a tropical river impacted by gold mining. In: In Environmental Research, 224. Elsevier BV, 115517. https://doi.org/10.1016/j.envres.2023.115517.
[33] Cortés-Gómez, A.A., Romero, D., Girondot, M., 2018. Carapace asymmetry: a possible biomarker for metal accumulation in adult olive ridleys marine turtles. Mar Pollut Bull 129 (s 1–2), 92–101. https://doi.org/10.1016/j.marpolbul.2018.02.020.
[34] Costa, P.G., Dal Pizzol, J.L., Zebral, Y.D., Bianchini, A., 2024. A reliable method to prepare milligram size environmental samples to quantify metal(loid)s by high-resolution graphite furnace atomic absorption spectrometry. In: In MethodsX, 13. Elsevier BV, 102896. https://doi.org/10.1016/j.mex.2024.102896.
[35] Coyle, P., Philcox, J.C., Carey, L.C., Rofe, A.M., 2002. Metallothionein: the multipurpose protein. CMLS Cell Mol Life Sci 59.
[36] Cunha, F.A.G., Forsberg, B.R., Vogt, R.C., Domingos, F.X.V., Marshall, B.G., Brito, B.C., de Sousa, O.P., Kasper, D., Santos, A.L.P., Ândrade, M., 2024. Mercury biomagnification in the food chain of a piscivorous turtle species (Testudines: Chelidae: *chelus fimbriata*) in the central Amazon, Brazil. Ecotoxicology 33 (s 4–5), 425–439. https://doi.org/10.1007/s10646-024-02756-w.
[37] da Silva, M.I.A., Lima, D., Venancio, L.P.R., da Silva, T.L., Domingos, C.R.B., de Almeida, E.A., 2025. Biochemical biomarker profiles of different organs of *phrynops geoffroanus* freshwater turtle (Testudines, Chelidae) reveal pollutant effects from an anthropized aquatic environment. Environ Res 279, 121847. https://doi.org/10.1016/j.envres.2025.121847.
[38] Dalla Valle, L., Nardi, A., Toni, M., Emera, D., Alibardi, L., 2009. Beta-keratins of turtle shell are glycine-proline-tyrosine rich proteins similar to those of crocodilians and birds. In: In Journal of Anatomy, 214. Wiley, pp. 284–300. https://doi.org/10.1111/j.1469-7580.2008.01030.x.
[39] Damos, P., 2016. Using multivariate cross correlations, granger causality and graphical models to quantify spatiotemporal synchronization and causality between pest populations. In: In BMC Ecology, 16. Springer Science and Business Media LLC. https://doi.org/10.1186/s12898-016-0087-7.
[40] Davidson, R., Harel, D., 1996. Drawing graphs nicely using simulated annealing. In: In ACM Transactions on Graphics, 15. Association for Computing Machinery (ACM, pp. 301–331. https://doi.org/10.1145/234535.234538.
[41] Day, R.D., Christopher, S.J., Becker, P.R., Whitaker, D.W., 2005. Monitoring Mercury in the loggerhead sea turtle, Caretta caretta. Environ Sci Technol 39 (2), 437–446. https://doi.org/10.1021/es049628q.
[42] Day, R.D., Segars, A.L., Arendt, M.D., Lee, A.M., Peden-Adams, M.M., 2007. Relationship of blood Mercury levels to health parameters in the loggerhead sea turtle (Caretta caretta). In: In Environmental Health Perspectives, 115. Environmental Health Perspectives, pp. 1421–1428. https://doi.org/10.1289/ehp.9918.
[43] De Vivero, M.M., De La Ossa, J.D., 2018. Feeding habits of *trachemys callirostris* (Gray, 1856) (Testudines: Emydidae), san benito abad, Sucre, Colombia. Indian J Sci Technol 11 (46), 1–4. https://doi.org/10.17485/ijst/2018/v11i46/137967.
[44] Dias, F.V.N., Garcês, L.M., de Oliveira, A.T., 2025. Contaminant levels and their effects on the American continent chelonian: a systematic review. Acta Zool 106, 247–264. https://doi.org/10.1111/azo.12550.
[45] Dias de Farias, D.S., Rossi, S., Bomfim, A.L.C., Fragoso, A.B.L., Santos-Neto, E.B., Silva, F.J.L., Navoni, J.A., Gavilán, S.A., Souza do Amaral, V., 2022. Bioaccumulation of total Mercury, copper, cadmium, silver, and selenium in Green turtles (*chelonia mydas*) stranded along the potiguar basin, northeastern Brazil. In: In Chemosphere, 299. Elsevier, 134331. https://doi.org/10.1016/j.chemosphere.2022.134331.
[46] Diaz, S.M., Palma, R.M., Muñoz, M.N., Becerra-Arias, C., Fernández Niño, J.A., 2020. Factors associated with high Mercury levels in women and girls from the mojana region, Colombia, 2013–2015. In: In International Journal of Environmental Research and Public Health, 17. MDPI AG, p. 1827. https://doi.org/10.3390/ijerph17061827.
[47] Díaz-Alarcón, J.A., Fonseca-Alfonso, P.M., Vergara-Gómez, I., Díaz-Lagos, M., Videira-Quintela, D., Montalvo, G., 2024. Assessment of potentially hazardous elements in soils of the Boyacá industrial corridor (Colombia) using GIS, multivariate statistical analysis, and geochemical indexes. In: In Ecotoxicology and Environmental Safety, 269. Elsevier BV, 115725. https://doi.org/10.1016/j.ecoenv.2023.115725.
[48] Dong, A., Dong, H., He, H., Dong, A., Yan, J., Huo, J., 2022. Effects of cadmium on kidney function of the freshwater turtles *mauremys reevesii*. In: In Biological Trace Element Research, 201. Springer Science and Business Media LLC, pp. 3000–3005. https://doi.org/10.1007/s12011-022-03397-y.
[49] dos Santos, R.L., de Sousa Correia, J.M., dos Santos, E.M., 2021. Freshwater aquatic reptiles (Testudines and Crocodylia) as biomonitor models in assessing environmental pollution by inorganic elements and the main analytical techniques used: a review. Environ Monit Assess 193, 498. https://doi.org/10.1007/s10661-021-09212-w.
[50] Drton, M., Maathuis, M.H., 2017. Structure learning in graphical modeling. In: In Annual Review of Statistics and Its Application, 4. Annual Reviews, pp. 365–393. https://doi.org/10.1146/annurev-statistics-060116-053803.
[51] Duarte, A., Spaan, R.S., Peterson, J.T., Pearl, C.A., Adams, M.J., 2025. Bayesian networks facilitate updating of species distribution and habitat suitability models. In: Ecological Modelling, 501. Elsevier, 110982. https://doi.org/10.1016/j.ecolmodel.2024.110982`.
[52] Dyrba, M., Mohammadi, R., Grothe, M.J., Kirste, T., Teipel, S.J., 2020. Gaussian graphical models reveal Inter-Modal and Inter-Regional conditional dependencies of brain alterations in Alzheimer's disease. Front Aging Neurosci 12. https://doi.org/10.3389/fnagi.2020.00099.
[53] Eisler, R., 1993. Zinc hazards to fish, wildlife, and invertebrates: a synoptic review (No. 26). US Department of the Interior, Fish and Wildlife Service. ⟨https://pubs.usgs.gov/publication/5200116⟩.
[54] Eisler, R., 2006. Mercury hazards to living organisms. CRC Press. https://doi.org/10.1201/9781420008838.
[55] Evers, D.C., Ackerman, J.T., Åkerblom, S., et al., 2024. Global Mercury concentrations in biota: their use as a basis for a global biomonitoring framework. Ecotoxicology 33, 325–396. https://doi.org/10.1007/s10646-024-02747-x.
[56] Farias da Fonseca, C.F., da Silva, I.J.S., da Silva Rodrigues, M., de Souza Silva, B. H., Soares, P.C., de Moura, G.J.B., de Oliveira, J.B., 2023. Evaluation of metal exposure through the composition of essential and toxic micro-minerals in freshwater turtles (*phrynops geoffroanus*) from a Brazilian river. Environ Sci Pollut Res 30 (19), 54871–54884. https://doi.org/10.1007/s11356-023-26127-w.
[57] Fayomi, A., Pantazis, Y., Tsagris, M., Wood, A.T.A., 2024. Cauchy robust principal component analysis with applications to high-dimensional data sets. In: In Statistics and Computing, 34. Springer Science and Business Media LLC. https://doi.org/10.1007/s11222-023-10328-x.
[58] Franzellitti, S., Locatelli, C., Gerosa, G., Vallini, C., Fabbri, E., 2004. Heavy metals in tissues of loggerhead turtles (Caretta caretta) from the northwestern adriatic sea. In: Comparative Biochemistry and Physiology, Part C: Toxicology & Pharmacology, 138. Elsevier, pp. 187–194. https://doi.org/10.1016/j.cca.2004.07.008.

[59] Fritz, U., Stuckas, H., Vargas-Ramírez, M., Hundsdörfer, A.K., Maran, J., Päckert, M., 2011. Molecular phylogeny of central and south American slider turtles: implications for biogeography and systematics (Testudines: Emydidae: Trachemys). In: In Journal of Zoological Systematics and Evolutionary Research, 50. Hindawi Limited, pp. 125–136. https://doi.org/10.1111/j.1439-0469.2011.00647.x.

[60] Fuentes-Lopez, K., Olivero-Verbel, J., Caballero-Gallardo, K., 2025. Presence of nematodes, Mercury concentrations, and liver pathology in carnivorous freshwater fish from la mojana, Sucre, Colombia: assessing fish health and potential human health risks. Arch Environ Contam Toxicol 88, 189–209. https://doi.org/10.1007/s00244-025-01117-w.

[61] Fujita, A., Sato, J.R., Demasi, M.A.A., Sogayar, M.C., Ferreira, C.E., Miyano, S., 2009. Comparing Pearson, spearman and Hoeffding's d measure for gene expression association analysis. In: In Journal of Bioinformatics and Computational Biology, 07. World Scientific Pub Co Pte Ltd, pp. 663–684. https://doi.org/10.1142/s0219720009004230.

[62] García-Fernández, A.J., Gómez-Ramírez, P., Martínez-López, E., Hernández-García, A., María-Mojica, P., Romero, D., Jiménez, P., Castillo, J.J., Bellido, J.J., 2009. Heavy metals in tissues from loggerhead turtles (Caretta caretta) from the southwestern Mediterranean (Spain). In: In Ecotoxicology and Environmental Safety, 72. Elsevier BV, pp. 557–563. https://doi.org/10.1016/j.ecoenv.2008.05.003.

[63] Garofalo, L., Sala, M., Focardi, C., Pasqualetti, P., Delfino, D., D'Onofrio, F., Droghei, B., Pasquali, F., Nicolini, V., Galli, F.S., Scaramozzino, P., Ubaldi, A., Russo, K., Neri, B., 2023. Monitoring of cadmium, lead, and Mercury levels in seafood products: a ten-year analysis. Foods 12 (15), 2871. https://doi.org/10.3390/foods12152871.

[64] Gibbons, J.W., Semlitsch, R.D., 1982. Survivorship and longevity of a Long-Lived vertebrate species: how long do turtles live? J Anim Ecol 51 (2), 523–527. https://doi.org/10.2307/3981.

[65] Golet, W.J., Haines, T.A., 2001. Snapping turtles (*chelydra serpentina*) as monitors for Mercury contamination of aquatic environments. In: Environmental Monitoring and Assessment, 71. Springer, pp. 211–220. https://doi.org/10.1023/A:1011802117198.

[66] Green, P.J., 1995. Reversible jump Markov chain Monte Carlo computation and Bayesian model determination. In: In Biometrika, 82. Oxford University Press (OUP, pp. 711–732. https://doi.org/10.1093/biomet/82.4.711.

[67] Green, A.D., Buhlmann, K.A., Hagen, C., Romanek, C., Gibbons, J.W., 2010. Mercury contamination in turtles and implications for human health. J Environ Health 72 (10), 14–23. ⟨http://www.jstor.org/stable/26329049⟩.

[68] Guan, N., Liu, T., Zhang, Y., Tao, D., Davis, L.S., 2019. Truncated Cauchy Non-Negative matrix factorization. IEEE Trans Pattern Anal Mach Intell 41 (1), 246–259. https://doi.org/10.1109/tpami.2017.2777841.

[69] Guimarães, A., 2024. Aquatic reptiles as model organisms to evaluate environmental pollution and biomonitoring. In The Handbook of Environmental Chemistry. Springer, Berlin, Heidelberg. https://doi.org/10.1007/698_2024_1183.

[70] Guirlet, E., Das, K., 2012. Cadmium toxicokinetics and bioaccumulation in turtles: trophic exposure of *trachemys scripta elegans*. Ecotoxicology 21 (1), 18–26. https://doi.org/10.1007/s10646-011-0758-2.

[71] Hastie, T.J., Tibshirani, R.J., Friedman, J.H., 2013. The elements of statistical learning: data mining, inference, and prediction. Springer Series in Statistics, 2nd Edn. Springer, New York, NY. https://doi.org/10.1007/978-0-387-84858-7.

[72] Hernández-Domínguez, C., Bjedov, D., Buelvas-Soto, J., Córdoba-Tovar, L., Bernal-Alviz, J., Marrugo-Negrete, J., 2025. Factors affecting arsenic and Mercury accumulation in fish from the Colombian Caribbean: a multifactorial approach using machine learning. Environ Res, 120761. https://doi.org/10.1016/j.envres.2025.120761.

[73] Hollander, M.A., Wolfe, D., Chicken, E., 2015. Nonparametric Statistical Methods. In Wiley Series in Probability and Statistics. Wiley. https://doi.org/10.1002/9781119196037.

[74] Hopkins, B.C., Willson, J.D., Hopkins, W.A., 2013. Mercury exposure is associated with negative effects on turtle reproduction. In: Environmental Science & Technology, 47. American Chemical Society (ACS), pp. 2416–2422. ⟨https://doi.org/10.1021/es304261s⟩.

[75] Hrizi, M., Jribi, I., Baracchini, C., Leignel, V., 2024. Metal bioaccumulation and biochemical responses in loggerhead turtles (Caretta caretta) from the gulf of Gabès (Tunisia). Environments 11, 214. https://doi.org/10.3390/environments11100214.

[76] Huo, J., Dong, A., Yan, J., Dong, A., 2020. Effects of cadmium on the gene transcription of the liver in the freshwater turtle (*chinemys reevesii*). In: In Environmental Science and Pollution Research, 27. Springer Science and Business Media LLC, pp. 8431–8438. https://doi.org/10.1007/s11356-019-07432-9.

[77] Huth, K.B.S., de Ron, J., Goudriaan, A.E., Luigjes, J., Mohammadi, R., van Holst, R.J., Wagenmakers, E.-J., Marsman, M., 2023. Bayesian analysis of Cross-Sectional networks: a tutorial in r and JASP. In: In Advances in Methods and Practices in Psychological Science, 6. SAGE Publications. https://doi.org/10.1177/25152459231193334.

[78] Huth, K.B.S., Keetelaar, S., Sekulovski, N., van den Bergh, D., Marsman, M., 2024. Simplifying Bayesian analysis of graphical models for the social sciences with easybgm: a user-friendly R-package (Advances.in). Adv /Psychol 2. https://doi.org/10.56296/aip00010.

[79] Ibrahem, L.I., Majeed, N.M., Obaid, S.M.H., Hashim, R.A., 2025. Mercury pollution and its impact on aquatic organisms. GSC Adv Res Rev 22 (03), 200–206. https://doi.org/10.30574/gsCarr.2025.22.3.0075.

[80] IDEAM. (2022). Datos de precipitación histórica. Instituto de Hidrología, Meteorología y Estudios Ambientales de Colombia (IDEAM). Recovered from https://www.ideam.gov.co .

[81] Jeong, H., Ali, W., Zinck, P., Souissi, S., Lee, J.S., 2024. Toxicity of methylmercury in aquatic organisms and interaction with environmental factors and coexisting pollutants: a review. In: In Science of the Total Environment, 943. Elsevier B.V. https://doi.org/10.1016/j.scitotenv.2024.173574.

[82] Johnson, D.B., 1977. Efficient algorithms for shortest paths in sparse networks. In: In Journal of the ACM, 24. Association for Computing Machinery (ACM, pp. 1–13. https://doi.org/10.1145/321992.321993.

[83] Kampalath, R., Gardner, S.C., Méndez-Rodríguez, L., Jay, J.A., 2006. Total and methylmercury in three species of sea turtles of baja california sur. In: Marine Pollution Bulletin, 52. Elsevier, pp. 1816–1823. https://doi.org/10.1016/j.marpolbul.2006.09.019.

[84] Kitana, N., Callard, I.P., 2008. Effect of cadmium on gonadal development in freshwater turtle (Trachemys scripta,Chrysemys picta) embryos. In: In Journal of Environmental Science and Health, Part A, 43. Informa UK Limited, pp. 262–271. https://doi.org/10.1080/10934520701792753.

[85] Klaassen, C.D., Liu, J., Choudhuri, S., 1999. METALLOTHIONEIN: an intracellular protein to protect against cadmium toxicity. Annu Rev Pharmacol Toxicol 39. ⟨www.annualreviews.org⟩.

[86] Kubo, W.K., de Oliveira, E.F., de Almeida Júnior, J.E., Sanches, A., de Oliveira, J. A., de Avelar São Pedro, V., 2025. Nuclear abnormalities in erythrocytes of black Spiny-Necked turtles (*acanthochelys spixii*) as evidence of agrochemical pollution in a monoculture landscape in Brazil. Chelonian Conserv Biol 24 (1), 125–135. https://doi.org/10.2744/CCB-1621.1.

[87] Kundu, S., Cheng, Y., Shin, M., Manyam, G., Mallick, B.K., Baladandayuthapani, V., 2018. Bayesian variable selection with graphical structure learning: applications in integrative genomics. PLoS ONE 13 (7), e0195070. https://doi.org/10.1371/journal.pone.0195070.

[88] Lee, Y., Song, J., 2021. Robustness of model averaging methods for the violation of standard linear regression assumptions. Commun Stat Appl Methods 28 (2), 189–204. https://doi.org/10.29220/csam.2021.28.2.189.

[89] Lettoof, D.C., Bateman, P.W., Aubret, F., Gagnon, M.M., 2020. The Broad-Scale analysis of metals, trace elements, organochlorine pesticides and polycyclic aromatic hydrocarbons in wetlands along an urban gradient, and the use of a high trophic Snake as a bioindicator. In: In Archives of Environmental Contamination and Toxicology, 78. Springer Science and Business Media LLC, pp. 631–645. https://doi.org/10.1007/s00244-020-00724-z.

[90] Li, J., Jia, L., Tian, Y., Chen, X., Liu, F., Huang, X., 2025. The combined effect of phosphorus forms and zinc on arsenic toxicity and bioaccumulation in Phaeodactylum tricornutum. Algal Research 75, 104097. https://doi.org/10.1016/j.algal.2025.104097.

[91] Li, B., Sun, Z., He, Q., Zhu, Y., Qin, Z.S., 2015. Bayesian inference with historical data-based informative priors improves detection of differentially expressed genes. In: In Bioinformatics, 32. Oxford University Press (OUP, pp. 682–689. https://doi.org/10.1093/bioinformatics/btv631.

[92] Liceaga-Correa, M.A., Uribe-Martínez, A., Cuevas, E., 2022. Ecological vulnerability of adult female marine turtles as indicators of opportunities for regional socioecosystem management in the Southern Gulf of Mexico. Sustainability. https://doi.org/10.3390/su16000000.

[93] Lynch, S.M., 2005. Bayesian statistics. In Encyclopedia of Social Measurement. Elsevier, pp. 135–144. https://doi.org/10.1016/b0-12-369398-5/00156-0.

[94] Maffucci, F., Caurant, F., Bustamante, P., Bentivegna, F., 2005. Trace element (Cd, Cu, Hg, Se, Zn) accumulation and tissue distribution in loggerhead turtles (Caretta caretta) from the Western Mediterranean Sea (Southern Italy). In: Chemosphere, 58. Elsevier, pp. 535–542. https://doi.org/10.1016/j.chemosphere.2004.09.032.

[95] Mair, P., Wilcox, R., 2020. Robust statistical methods in r using the WRS2 package. In: In Behavior Research Methods, 52. Springer Science and Business Media LLC, pp. 464–488. https://doi.org/10.3758/s13428-019-01246-w.

[96] Malekmohammadi, B., Uvo, C.B., Tayebzadeh Moghadam, N., Noori, R., Abolfathi, S., 2023. Environmental risk assessment of wetland ecosystems using Bayesian belief networks. Hydrology 10 (1), 16. https://doi.org/10.3390/hydrology10010016.

[97] Malik, R.N., Ghaffar, B., Hashmi, M.Z., 2013. Trace metals in Ganges soft-shell turtle (*aspideretes gangeticus*) from two barrage: baloki and rasul, Pakistan. Environ Sci Pollut Res 20 (11), 8263–8273. https://doi.org/10.1007/s11356-013-1805-8.

[98] Marrugo-Negrete, J., Benitez, L.N., Olivero-Verbel, J., 2008. Distribution of Mercury in several environmental compartments in an aquatic ecosystem impacted by gold mining in Northern Colombia. In: In Archives of Environmental Contamination and Toxicology, 55. Springer Science and Business Media LLC, pp. 305–316. https://doi.org/10.1007/s00244-007-9129-7.

[99] Marrugo-Negrete, J., Durango-Hernández, J., Calao-Ramos, C., Urango-Cárdenas, I., Díez, S., 2019. Mercury levels and genotoxic effect in caimans from tropical ecosystems impacted by gold mining. In: In Science of The Total Environment, 664. Elsevier BV, pp. 899–907. https://doi.org/10.1016/j.scitotenv.2019.01.340.

[100] Marrugo-Negrete, J., Pinedo-Hernández, J., Díez, S., 2017. Assessment of heavy metal pollution, spatial distribution and origin in agricultural soils along the Sinú river basin, Colombia. In: In Environmental Research, 154. Elsevier BV, pp. 380–388. https://doi.org/10.1016/j.envres.2017.01.021.

[101] Marrugo-Negrete, J., Pinedo-Hernández, J., Combatt, E.M., Bravo, A.G., Díez, S., 2019. Flood-induced metal pollution in the topsoil of floodplain agricultural soils:

a case-study in Colombia. In land degradation &amp. In: Development, 30. Wiley, pp. 2139–2149. https://doi.org/10.1002/ldr.3398.
[102] Marrugo-Negrete, J., Pinedo-Hernández, J., Combatt, E.M., Bravo, A.G., Díez, S., 2019. Flood-induced metal pollution in the topsoil of floodplain agricultural soils: a case-study in Colombia. Environ Toxicol Chem 38 (12), 2755–2765. https://doi.org/10.1002/etc.4398.
[103] Marrugo-Negrete, J., Pinedo-Hernández, J., Marrugo-Madrid, S., Díez, S., 2020. Assessment of trace element pollution and ecological risks in a river basin impacted by mining in Colombia. In: In Environmental Science and Pollution Research, 28. Springer Science and Business Media LLC, pp. 201–210. https://doi.org/10.1007/s11356-020-10356-4.
[104] Marrugo-Negrete, J., Pinedo-Hernández, J., Marrugo-Madrid, S., Gámez-Flórez, W., Díez, S., 2024. Evaluating ecological risks and metal bioavailability in post-dredging sediments of a wetland affected by artisanal gold mining. Sci Total Environ 955, 176309. https://doi.org/10.1016/j.scitotenv.2024.176309.
[105] Marrugo-Negrete, J., Verbel, J.O., Ceballos, E.L., Benitez, L.N., 2008. Total Mercury and methylmercury concentrations in fish from the mojana region of Colombia. In: In Environmental Geochemistry and Health, 30. Springer Science and Business Media LLC, pp. 21–30. https://doi.org/10.1007/s10653-007-9104-2.
[106] Martín-del-Campo, R., Bárcenas-Ibarra, A., Lund, G., Rodríguez-Ríos, D., Yong-Villalobos, L., García-Hernández, J., García-Gasca, A., 2019. Mercury concentration, DNA methylation, and mitochondrial DNA damage in olive ridley sea turtle embryos with schistosomus reflexus syndrome. In: In Veterinary Pathology, 56. SAGE Publications, pp. 940–949. https://doi.org/10.1177/0300985819868649.
[107] Martínez, C.A., Khare, K., Rahman, S., Báez, G.M., 2025. Graphical model selection to infer the partial correlation network of allelic effects in genomic prediction with an application in dairy cattle. In Journal of Animal Breeding and Genetics. Wiley. https://doi.org/10.1111/jbg.12921.
[108] Merleau, L.-A., Goutte, A., Olivier, A., Vittecoq, M., Bustamante, P., Leray, C., Lourdais, O., 2024. Blood levels of metallic trace elements are influenced by sex, age and habitat in the european pond turtle (*emys orbicularis*). Sci Total Environ 957, 177487. https://doi.org/10.1016/j.scitotenv.2024.177487.
[109] Meyer, E., Eagles-Smith, C.A., Sparling, D., Blumenshine, S., 2014. Mercury exposure associated with altered plasma thyroid hormones in the declining Western pond turtle (*emys marmorata*) from california mountain streams. In: Environmental Science & Technology, 48. American Chemical Society (ACS), pp. 2989–2996. https://doi.org/10.1021/es4050538.
[110] Meza-Martínez, M., Ossa-Velázquez, J.D. La, Hernández-Gómez, J., Marrugo-Negrete, J., 2020. Total Mercury in liver of *trachemys callirostris* (Gray, 1856) (Testudines: Emydidae) in three areas of la mojana, Sucre-Colombia. Rev U D C A Actual Divulg Cient 23 (1). https://doi.org/10.31910/rudca.v23.n1.2020.1239.
[111] Mohammadi, A., Abegaz, F., Heuvel, E., Wit, E.C., 2016. Bayesian modelling of dupuytren disease by using Gaussian copula graphical models. In: Journal of the Royal Statistical Society Series C: Applied Statistics, 66. Oxford University Press (OUP, pp. 629–645. https://doi.org/10.1111/rssc.12171.
[112] Mohammadi, R., Massam, H., Letac, G., 2021. Accelerating Bayesian structure learning in sparse Gaussian graphical models. In: Journal of the American Statistical Association, 118. Informa UK Limited, pp. 1345–1358. https://doi.org/10.1080/01621459.2021.1996377.
[113] Mohammadi, R., Wit, E.C., 2019. BDgraph: an r package for Bayesian structure learning in graphical models. J Stat Softw 89 (3), 1–30. https://doi.org/10.18637/jss.v089.i03.
[114] Morales-Betancourt, M.A., C.A. Lasso, V.P. Páez y B. C. Bock. 2015. Libro rojo de reptiles de Colombia (2015). Instituto de Investigación de Recursos Biológicos Alexander von Humboldt (IAvH), Universidad de Antioquia. Bogotá, D. C., Colombia. 258 pp. 〈http://catalogo.humboldt.org.co/cgi-bin/koha/opac-detail.pl?biblionumber=18728〉.
[115] Nardini, A., Franco-Idarraga, F., 2016. A qualitative Hydro-Geomorphic prediction of the destiny of the mojana region (Magdalena-Cauca Basin, Colombia), to inform large scale decision making. In: In Resources, 5. MDPI AG, p. 22. https://doi.org/10.3390/resources5030022.
[116] Olivero-Verbel, J., Caballero-Gallardo, K., Negrete-Marrugo, J., 2011. Relationship between localization of gold mining areas and hair Mercury levels in people from bolivar, north of Colombia. In: In Biological Trace Element Research, 144. Springer Science and Business Media LLC, pp. 118–132. https://doi.org/10.1007/s12011-011-9046-5.
[117] Ortiz-Santaliestra, M.E., Rodríguez, A., Pareja-Carrera, J., Mateo, R., Martinez-Haro, M., 2019. Tools for non-invasive sampling of metal accumulation and its effects in Mediterranean pond turtle populations inhabiting mining areas. Chemosphere 231, 194–206. https://doi.org/10.1016/j.chemosphere.2019.05.082.
[118] Páez, V.P., Bock, B.C., Alzate-Estrada, D.A., Barrientos-Muñoz, K.G., Cartagena-Otálvaro, V.M., Echeverry-Alcendra, A., Gómez-Rincón, M.T., Ramírez-Gallego, C., del Río, J.S., & Vallejo-Betancur, M.M. (2022). Turtles of Colombia: An annotated analysis of their diversity, distribution, and conservation status. Amphibian & Reptile Conservation, 16(1), 106–135 (e306). 〈https://amphibian-reptile-conservation.org/pdfs/Volume/Vol_16_no_1/ARC_16_1_〉[General_Section]_106-135_e306.pdf.
[119] Pavlopoulos, G.A., Secrier, M., Moschopoulos, C.N., Soldatos, T.G., Kossida, S., Aerts, J., Schneider, R., Bagos, P.G., 2011. Using graph theory to analyze biological networks. BioData Min 4 (1). https://doi.org/10.1186/1756-0381-4-10.
[120] Pearson, R.K., 2002. Outliers in process modeling and identification. In: In IEEE Transactions on Control Systems Technology, 10. Institute of Electrical and Electronics Engineers (IEEE, pp. 55–63. https://doi.org/10.1109/87.974338.
[121] Peng, Y., Yu, G.I., 2024. Prediction of the impact of ecological restoration technology on the restoration of heavy metal pollution in agricultural soil. Environmental Challenges 9, 100331. https://doi.org/10.1080/24749508.2024.2328900.
[122] Pereira da Costa Araújo, A., Lima, V.S., Emmanuela de Andrade Vieira, J., Mesak, C., Malafaia, G., 2019. First report on the mutagenicity and cytotoxicity of zno nanoparticles in reptiles. In: Chemosphere, 235. Elsevier BV, pp. 556–564. https://doi.org/10.1016/j.chemosphere.2019.06.164.
[123] Peterson, E.E., Hanks, E.M., Hooten, M.B., Ver Hoef, J.M., Fortin, M., 2019. Spatially structured statistical network models for landscape genetics. In: Ecological Monographs, 89. Wiley. https://doi.org/10.1002/ecm.1355.
[124] Pignati, M.T., Pezzuti, J.C.B., Souza, L.C. de, Lima, M. de O., Pignati, W.A., Mendes, R. de A., 2018. Assessment of Mercury concentration in turtles (*podocnemis unifilis*) in the Xingu river basin, Brazil. Int J Environ Res Public Health 15 (6). https://doi.org/10.3390/ijerph15061185.
[125] Prieto, A., Zuloaga, O., Usobiaga, A., Etxebarria, N., Fernández, L.A., Marcic, C., de Diego, A., 2008. Simultaneous speciation of methylmercury and butyltin species in environmental samples by headspace-stir bar sorptive extraction–thermal desorption–gas chromatography–mass spectrometry. Journal of Chromatography A 1185 (1), 130–138. https://doi.org/10.1016/j.chroma.2008.01.046.
[126] R Core Team, 2024. R: A Language and Environment for Statistical Computing. R Foundation for Statistical Computing, Vienna. https://www.R-project.org.
[127] Ramachandran, A.V., Kinariwala, R.V., Shah, R.V., 1985. Haematopoiesis and regeneration: changes in the liver, spleen, bone marrow and hepatic iron content during tail regeneration in the scincid lizard, *mabuya carinata* (Boulenger). AmphibReptil 6 (4), 377–386. 〈https://brill.com/view/journals/amre/6/4/article-p377_6.xml〉.
[128] Rendón-Valencia, B., Zapata, L.M., Bock, B.C., Páez, V.P., Palacio, J.A., 2014. Niveles de mercurio en huevos, embriones y neonatos de *trachemys callirostris* (Testudines, Emydidae). Acta Biológica Colomb 19 (3), 499–506.
[129] Restrepo, A., Páez, V.P., Bock, B.C., Daza, J.M., Díazgranados, I., 2014. Catálogo de anfibios y reptiles de Colombia. Trac callirostris (Gray 1856) Icotea Hicotea Jicotea Galápago AsocóN Colomb De Herpetología ACH 2 (2), 7–12. 〈https://bibliotecadigital.udea.edu.co/bitstream/10495/33403/1/RestrepoAdriana_2014_Trachemys-callirostris.pdf〉.
[130] Restrepo, A., Piñeros, V.J., Páez, V.P., 2006. Nest site selection by Colombian slider turtles, trachemys callirostris callirostris (Testudines: Emydidae), in the mompos depression, Colombia. Chelonian Conserv Biol 5 (2), 249–254. https://doi.org/10.2744/1071-8443(2006)5[249:nssbcs]2.0.co;2.
[131] Restrepo, J.D., Syvitski, J.P.M., 2006. Assessing the effect of natural controls and land use change on sediment yield in a major andean river: the Magdalena drainage basin, Colombia. In: AMBIO: A Journal of the Human Environment, 35. Royal Swedish Academy of Sciences, pp. 65–74. https://doi.org/10.1579/0044-7447(2006)35[65:ateonc]2.0.co;2.
[132] Riaño, C., Ortiz-Ruiz, M., Pinto-Sánchez, N.R., Gómez-Ramírez, E., 2020. Effect of glyphosate (Roundup Active®) on liver of tadpoles of the Colombian endemic frog *dendropsophus molitor* (amphibia: Anura). In: Chemosphere, 250. Elsevier BV, 126287. https://doi.org/10.1016/j.chemosphere.2020.126287.
[133] Riva-Murray, K., Bradley, P.M., Brigham, M.E., 2020. Methylmercury—total Mercury ratios in predator and primary consumer insects from adirondack streams (New York, USA). Ecotoxicology 29 (10), 1644–1658. https://doi.org/10.1007/s10646-020-02191-7.
[134] Romero-Núñez, S.E., Marrugo-Negrete, J.L., Rios, J.E.A., Hadad, H.R., Maine, M. A., 2011. Hg, cu, pb, cd, and zn accumulation in macrophytes growing in tropical wetlands. In: Water, Air, & Soil Pollution, 216. Springer Science and Business Media LLC., pp. 361–373. https://doi.org/10.1007/s11270-010-0538-2
[135] Rúa-Cardona, A.F., Flórez Molina, M.T., Palacio Baena, J., 2013. Variations of seasonal and spatial hg, pb, cr and organic matter contents in ayapel flood plain lake sediments, Córdoba, northwest Colombia. Revista Facultad de Ingeniería Universidad de Antioquia. Universidad de Antioquia, pp. 244–255. https://doi.org/10.17533/udea.redin.18153.
[136] Sah, P., Singh, L.O., Clauset, A., Bansal, S., 2014. Exploring community structure in biological networks with random graphs. In: BMC Bioinformatics, 15. Springer Science and Business Media LLC. https://doi.org/10.1186/1471-2105-15-220.
[137] Saidon, N.B., Szabó, R., Budai, P., Lehel, J., 2024. Trophic transfer and biomagnification potential of environmental contaminants (heavy metals) in aquatic ecosystems. In: Environmental Pollution, 340. Elsevier BV, 122815. https://doi.org/10.1016/j.envpol.2023.122815.
[138] Sakai, H., Saeki, K., Ichihashi, H., Suganuma, H., Tatsukawa, R., 2000. Species-specific distribution of heavy metals in tissues and organs of loggerhead turtle (Caretta caretta) and Green turtle (*chelonia mydas*) from Japanese coastal waters. In: Marine Pollution Bulletin, 40. Elsevier Science Ltd, pp. 701–709. https://doi.org/10.1016/S0025-326X(00)00008-4.
[139] Seidel, M.E., 2002. Taxonomic observations on extant species and subspecies of slider turtles, genus trachemys. J Herpetol 36 (2), 285–292. https://doi.org/10.2307/1566003.
[140] Sekulovski, N., Keetelaar, S., Huth, K., Wagenmakers, E.-J., van Bork, R., van den Bergh, D., Marsman, M., 2024. Testing conditional independence in psychometric networks: an analysis of three Bayesian methods. In: Multivariate Behavioral Research, 59. Informa UK Limited, pp. 913–933. https://doi.org/10.1080/00273171.2024.2345915.

[141] Serra, F., Iaccarino, D., Fiorito, F., Di Nocera, F., Esposito, M., Cerracchio, C., Esposito, E., Lambiase, S., Degli Uberti, B., Lucifora, G., De Carlo, E., Fusco, G., Amoroso, M.G., 2023. Investigation on anthropogenic and opportunistic factors relevant to the incidence of stranded loggerhead sea turtle Caretta caretta along south tyrrhenian coasts. Front Mar Sci 10, 1116804. https://doi.org/10.3389/fmars.2023.1116804.

[142] Sherwood, N., Wu, M., Weis, P., 2018. Mercury contamination in diamondback terrapins in new jersey. In: Environmental Management, 62. Springer Science and Business Media LLC, pp. 756–765. https://doi.org/10.1007/s00267-018-1075-9.

[143] Smid, S.C., McNeish, D., Miočević, M., van de Schoot, R., 2019. Bayesian versus frequentist estimation for structural equation models in small sample contexts: a systematic review. In: Structural Equation Modeling: A Multidisciplinary Journal, 27. Informa UK Limited, pp. 131–161. https://doi.org/10.1080/10705511.2019.1577140.

[144] Stanford, C.B., Iverson, J.B., Rhodin, A.G.J., van Dijk, P.P., Mittermeier, R.A., Kuchling, G., Vogt, R.C., Walde, A.D., 2020. Turtles and tortoises are in trouble. Curr Biol 30 (12), R721–R735. https://doi.org/10.1016/j.cub.2020.04.088.

[145] Stark, A.A.P., Corcini, C.D., Oliveras, M.Y., Bianchini, A., Acosta, I.B., Costa, P.G., da Silva Zani, G., Junior, A.S.V., França, R.T., 2024. *trachemys dorbigni* as a metal (loid) bioindicator: a study in rural and urban areas. Environ Monit Assess 196 (12), 1207. https://doi.org/10.1007/s10661-024-13384-6.

[146] Suzuki, K.T., Miyamoto, E., Tanaka, Y., Kawamura, R., Yamamura, M., 1984. Effect of diet on urinary and fecal excretion of cadmium, copper, and zinc from rats preaccumulated heavily with cadmium. In: Archives of Environmental Contamination and Toxicology, 13. Springer Science and Business Media LLC, pp. 621–626. https://doi.org/10.1007/bf01056341.

[147] Tarra, J.A., Restrepo, O.J., Veiga, M.M., 2022. Coexistence between conventional alluvial mining and artisanal mining to deal with problems associated with informality in the lower Nechí river Basin-Colombia. Resour Policy 78, 102821. https://doi.org/10.1016/j.resourpol.2022.102821.

[148] Tibshirani, R., Walther, G., Hastie, T., 2001. Estimating the number of clusters in a data set via the gap statistic. In: Journal of the Royal Statistical Society Series B: Statistical Methodology, 63. Oxford University Press (OUP, pp. 411–423. https://doi.org/10.1111/1467-9868.00293.

[149] Traag, V.A., Waltman, L., van Eck, N.J., 2019. From louvain to Leiden: guaranteeing well-connected communities. In: Scientific Reports, 9. Springer Science and Business Media LLC. https://doi.org/10.1038/s41598-019-41695-z.

[150] Universidad de Córdoba - Instituto de Investigaciones Biológicas Alexander von Humboldt (2019). Vertebrados de los humedales de La Mojana, Colombia. ⟨http://i2d.humboldt.org.co/ceiba/resource.do?r=vertebrados_mojana_2018⟩.

[151] USEPA. (1998). United state environmental protection agency. Method 7473 (SW-846). Mercury in Solids and Solutions by Thermal Decomposition, Amalgamation, and Atomic Absorption Spectrophotometry (Methods). ⟨https://www.epa.gov/sites/default/files/2015-12/documents/7473.pdf⟩.

[152] USEPA (2007). Method 3051A (SW-846): Microwave Assisted Acid Digestion of Sediments, Sludges, and Oils," Revision 1. Washington, DC. ⟨https://www.epa.gov/sites/default/files/2015-12/documents/3051a.pdf⟩.

[153] Vogels, L., Mohammadi, R., Schoonhoven, M., Birbil, Ş.İ., 2024. Bayesian structure learning in undirected Gaussian graphical models: literature review with empirical comparison. J Am Stat Assoc 1–33. https://doi.org/10.1080/01621459.2024.2395504.

[154] Vogt, R.C., 2016. Freshwater turtles. Reptile Ecology and Conservation. Oxford University Press, pp. 168–180. https://doi.org/10.1093/acprof:oso/9780198726135.003.0013.

[155] Wang, W.C., Mao, H., Ma, D.D., Yang, W.X., 2014. Characteristics, functions, and applications of metallothionein in aquatic vertebrates. In: Frontiers in Marine Science, 1. Issue AUG). Frontiers Media S. A. https://doi.org/10.3389/fmars.2014.00034.

[156] Wang, H., Sun, L., Liu, Z., Luo, Q., 2017. Spatial distribution and seasonal variations of heavy metal contamination in surface waters of liaohe river, northeast China. In: Chinese Geographical Science, 27. Springer Science and Business Media LLC, pp. 52–62. https://doi.org/10.1007/s11769-017-0846-1.

[157] Wang, M., Wang, H., Zheng, H., 2022. A mini review of node centrality metrics in biological networks. Int J Netw Dyn Intell 99–110. https://doi.org/10.53941/ijndi0101009.

[158] Wilcox, R.R., 2013. Introduction to robust estimation and hypothesis testing, 3rd ed. Academic press. https://doi.org/10.1016/C2010-0-67044-1.

[159] Wilcox, R.R., 2023. A guide to robust statistical methods. Springer Nature Switzerland. https://doi.org/10.1007/978-3-031-41713-9.

[160] Wilcox, R.R., Tian, T.S., 2011. Measuring effect size: a robust heteroscedastic approach for two or more groups. In: Journal of Applied Statistics, 38. Informa UK Limited, pp. 1359–1368. https://doi.org/10.1080/02664763.2010.498507.

[161] World Health Organization - WHO, 2008. Guidance for identifying populations at risk from Mercury exposure. ⟨https://wedocs.unep.org/20.500.11822/31566⟩.

[162] Wuchty, S., Ravasz, E., Barabási, A.L., 2006. The architecture of biological networks. In: Deisboeck, T.S., Kresh, J.Y. (Eds.), Complex Systems Science in Biomedicine. Topics in Biomedical Engineering International Book Series. Springer, Boston, MA. https://doi.org/10.1007/978-0-387-33532-2_5.

[163] Wyneken, J. (2001). The anatomy of sea turtles. U.S. Department of Commerce - NOAA Technical Memorandum NMFS-SEFSC-470. Washington, D.C: NOAA. 1–172. ⟨https://repository.library.noaa.gov/view/noaa/8502⟩.

[164] Xu, H., Zhang, L., Li, P., Zhu, F., 2022. Outlier detection algorithm based on k-nearest neighbors-local outlier factor. In: Journal of Algorithms & Computational Technology, 16. SAGE Publications. ⟨https://doi.org/10.1177/17483026221078111⟩.

[165] Yan Ng, C.K.Y., Lam, J.C.W., Zhang, X.H., Gu, H.X., Li, T.H., Ye, M.Bin, Xia, Z.R., Zhang, F.Y., Duan, J.X., Wang, W.X., Lam, I.K.S., Balazs, G.H., Lam, P.K.S., Murphy, M.B., 2018. Levels of trace elements, methylmercury and polybrominated diphenyl ethers in foraging Green turtles in the south China region and their conservation implications. Environ Pollut 234, 735–742. https://doi.org/10.1016/j.envpol.2017.11.100.

[166] Yang, L., Wei, Y., Gao, S., Wang, Q., Chen, J., Tang, B., Bian, X., 2022. Effect of copper nanoparticles and ions on epididymis and spermatozoa viability of Chinese Soft-Shelled turtles *pelodiscus sinensis*. In: In Coatings, 12. MDPI AG, p. 110. https://doi.org/10.3390/coatings12020110.

[167] Yu, S., Halbrook, R.S., Sparling, D.W., Colombo, R., 2011. Metal accumulation and evaluation of effects in a freshwater turtle. In: In Ecotoxicology, 20. Springer Science and Business Media LLC, pp. 1801–1812. https://doi.org/10.1007/s10646-011-0716-z.

[168] Zapata, L.M., Bock, B.C., Palacio, J.A., 2014. Mercury concentrations in tissues of Colombian slider turtles, *t. callirostris*, from Northern Colombia. In: In Bulletin of Environmental Pollution and Toxicology, 92. Springer Science and Business Media LLC, pp. 562–566. https://doi.org/10.1007/s00128-014-1198-5.

[169] Zapata, L.M., Bock, B.C., Orozco, L.Y., Palacio, J.A., 2016. Application of the micronucleus test and comet assay in *t. callirostris* erythrocytes as a model for in situ genotoxic monitoring. In: In Ecotoxicology and Environmental Safety, 127. Elsevier BV, pp. 108–116. https://doi.org/10.1016/j.ecoenv.2016.01.016.

[170] Zhao, L., Liao, M., Li, L., Chen, L., Zhang, T., Li, R., 2024. Cadmium activates the innate immune system through the AIM2 inflammasome. Chemico-Biological Interactions 399, 111122. https://doi.org/10.1016/j.cbi.2024.111122.

[171] Zitzmann, S., Lüdtke, O., Robitzsch, A., Hecht, M., 2020. On the performance of Bayesian approaches in small samples: a comment on smid, McNeish, miocevic, and van de schoot (2019). in. In: Structural Equation Modeling: A Multidisciplinary Journal, 28. Informa UK Limited, pp. 40–50. https://doi.org/10.1080/10705511.2020.1752216.

[172] Zondervan-Zwijnenburg, M., Peeters, M., Depaoli, S., Van de Schoot, R., 2017. Where do priors come from? Applying guidelines to construct informative priors in small sample research. Res Hum Dev 14 (4), 305–320. https://doi.org/10.1080/15427609.2017.1370966.

Portada revista – Journal of Hazardous Materials

ScienceDirect

Journals & Books | Help | Search | My account

Journal of Hazardous Materials

Supports open access

24.6 CiteScore | 11.3 Impact Factor

Articles & Issues | About | Publish | Order journal | Search in this journal | Submit your article | Guide for authors

About the journal

The Journal of Hazardous Materials is an international forum that advances world class research by publishing articles in the areas of Environmental Science and Engineering. We publish full-length research papers, review articles, and perspectives that improve our understanding of the hazards and ...

View full aims & scope

Article publishing options

Open Access

Article Publishing Charge (APC): USD 4900 (excluding taxes). The amount you pay may be reduced during submission if applicable.

Review this journal's open access policy.

Subscription

No publication fee charged to authors, and published articles are immediately available to subscribers.

4 days	33 days	83 days	2 days	View all insights
Time to first decision	Review time	Submission to acceptance	Acceptance to publication	

Prueba de indexación SJR - **Journal of Hazardous Materials**

SJR SI EPI SCImago

SJR Scimago Journal & Country Rank

Enter Journal Title,

Home | Journal Rankings | Journal Value | Country Rankings | Viz Tools | Help | About Us

Journal of Hazardous Materials

COUNTRY

Netherlands

Universities and research institutions in Netherlands

Media Ranking in Netherlands

SUBJECT AREA AND CATEGORY

Environmental Science
- Environmental Chemistry
- Environmental Engineering
- Health, Toxicology and Mutagenesis
- Pollution
- Waste Management and Disposal

PUBLISHER

Elsevier B.V.

SJR 2024

3.078 Q1

H-INDEX

375